The Journal of Immunology

B Cells in Teleost Fish Act as Pivotal Initiating APCs in Priming Adaptive Immunity: An Evolutionary Perspective on the Origin of the B-1 Cell Subset and B7 Molecules

Lv-yun Zhu, Ai-fu Lin, Tong Shao, Li Nie, Wei-ren Dong, Li-xin Xiang and Jian-zhong Shao

J Immunol 2014; 192:2699-2714; Prepublished online 14 February 2014;
doi: 10.4049/jimmunol.1301312
http://www.jimmunol.org/content/192/6/2699

The Journal of Immunology is published twice each month by
The American Association of Immunologists, Inc.,
1451 Rockville Pike, Suite 650, Rockville, MD 20852

Print ISSN: 0022-1767 Online ISSN: 1550-6606.

B Cells in Teleost Fish Act as Pivotal Initiating APCs in Priming Adaptive Immunity: An Evolutionary Perspective on the Origin of the B-1 Cell Subset and B7 Molecules

Lv-yun Zhu, Ai-fu Lin, Tong Shao, Li Nie, Wei-ren Dong, Li-xin Xiang, and Jian-zhong Shao

The long-held paradigm that B cells cannot uptake nonspecific particulate Ags for the initiation of primary adaptive immunity has been challenged by the recent discovery that teleost B cells have potent phagocytic and microbicidal abilities. This discovery provides preliminary clues that primitive B cells might act as initiating APCs in priming adaptive immunity. In this study, zebrafish B cells clearly showed a potent Ag-presenting ability to both soluble Ags and bacterial particles to prime naive $CD4^+$ T cell activation. This finding demonstrates the innate-like nature of teleost B cells in the interface of innate and adaptive immunity, indicating that they might consist of a major population of initiating APCs whose performance is similar to that of dendritic cells. Given the functional similarities between teleost B cells and the mammalian B-1 subset, we hypothesize that B-1 lineage and teleost B cells might originate from a common ancestor with potent phagocytic and initiating APC capacities. In addition, CD80/86 and CD83 costimulatory signals were identified as being essential for B cell–initiated adaptive immunity. This result suggests that the costimulatory mechanism originated as early as the origin of adaptive immunity and is conserved throughout vertebrate evolution. In fish, only a single CD80/86 copy exists, which is similar to mammalian CD86 rather than to CD80. Thus, CD86 might be a more primordial B7 family member that originated from fish. This study provides valuable insights into the evolutionary history of professional APCs, B cell lineages, and the costimulatory mechanism underlying adaptive immunity as a whole. ***The Journal of Immunology*****, 2014, 192: 2699–2714.**

It has long been recognized that B cells in mammals are one of the professional APCs, in addition to their performance as Ab-producing cells (1). As APCs, B cells uptake specific soluble Ags through BCR-mediated endocytosis, thereby presenting Ags to cognate Ag-specific $CD4^+$ T cells by MHC class II (MHC II) and costimulatory molecules (2). However, their presenting ability with regard to nonspecific particle Ags, such as bacterial pathogen particles, is negligible (3). Therefore, B cells are believed to be mainly engaged in the activation of memory $CD4^+$ T cells in secondary immune responses and have not been recognized as initiating APCs for naive $CD4^+$ T cells in priming adaptive immunity as dendritic cells (DCs) and macrophages have been.

However, this long-held paradigm has largely been challenged by the recent discovery that B cells in fish have potent phagocytic ability for nonspecific particle Ags and strong microbicidal activity; similar observations were reported in amphibians and reptiles (4–6). These results imply that B cells in primitive vertebrates, similar to DCs and macrophages in mammals, may act as pivotal initiating APCs in priming naive T cells. Clarification of this hypothesis may benefit not only to the functional characterization of B cells in ancient vertebrates, from which adaptive immunity originates, but also to the understanding of the evolutionary history of B cell populations, such as the origin of the B-1 subset, one of the major subgroups of the B cell repertoire in mammals. In fact, B-1 cells have primitive features that are different from those of conventional B-2 cells (7, 8). For instance, they produce IgM as natural Abs and uptake nonspecific endogenous Ags for inducing and maintaining immunological tolerance (9). Particularly, they recently were confirmed to have phagocytic and microbicidal abilities similar to those of IgM^+ B cells in fish and were suggested to function as initiating APCs (10, 11). These observations suggest that B-1 cells represent a more primitive population that resembles, in many aspects, the B cells in ancient vertebrates, such as fish. Therefore, a close evolutionary relationship might exist between B-1 cells in mammals and B cells in primitive vertebrates. To explore this possibility, different lower vertebrate research models, particularly teleost fish, the species with the most primitive adaptive immunity, are integral participants. Thus, the functional performance of teleost B cells in the initiation of adaptive immunity is requisite to this understanding.

College of Life Sciences, Zhejiang University, Hangzhou 310058, People's Republic of China; Key Laboratory for Cell and Gene Engineering of Zhejiang Province, Hangzhou 310058, People's Republic of China; and Key Laboratory of Animal Virology of Ministry of Agriculture, Hangzhou 310058, People's Republic of China

Received for publication May 16, 2013. Accepted for publication January 8, 2014.

This work was supported by grants from the High-Technology Research and Development Program of China (863) (2012AA092202), the National Basic Research Program of China (973) (2012CB114404, 2012CB114402), the National Natural Science Foundation of China (31072234, 31172436, 31272691, 31372554), the Program for Key Innovative Research Team of Zhejiang Province (2010R50026), the Scientific Research Fund of Zhejiang Provincial Science and Technology Department (2013C12907-9), and a Scholarship Award for Excellent Doctoral Student granted by the Ministry of Education.

The sequences presented in this article have been submitted to GenBank (http://www.ncbi.nlm.nih.gov/genbank/) under accession numbers KC414844 and KC414845.

Address correspondence and reprint requests to Prof. Jian-zhong Shao and Assoc. Prof. Li-xin Xiang, Zhejiang University, YuHangTang Road 888, Hangzhou 310058, Zhejiang, People's Republic of China. E-mail addresses: xianglx@zju.edu.cn (J.-z.S.) and shaojz@zju.edu.cn (L.-x.X.)

The online version of this article contains supplemental material.

Abbreviations used in this article: $CD4^+$ T_{KLH}, KLH-stimulated $CD4^+$ T cell; $CD4^+$ $T_{V.A.}$, *Vibrio alginolyticus*–stimulated $CD4^+$ T cell; CsA, cyclosporin A; DC, dendritic cell; FITC-KLH, FITC conjugated to KLH; FITC-V.A., FITC conjugated to *V. alginolyticus*; HK, head kidney; HKL, head kidney lymphocyte; IgC-like, Ig C region like; IgV-like, Ig V region like; KLH, keyhole limpet hemocyanin; LV, lentivirus; MHC II, MHC class II; mIgM, membrane IgM; NGS, *N*-linked glycosylation site; siRNA, small interfering RNA.

The most critical event in the activation of adaptive immunity is cell-to-cell signal exchanges between APCs and T cells, which deeply influence the profile and extent of the adaptive immunity (12). Costimulatory signals are indispensable for this process. Among the known costimulatory molecules, CD80 (B7-1), CD86 (B7-2), and CD83 are three of the most important and well-characterized in mammals (13–15). They provide regulatory signals to stimulate naive T cells or attenuate the strength of T cell responses by interacting with their reciprocal receptors, such as CD28 and CTLA-4 (16). Despite numerous studies in mammals, little is known about their occurrence and functional performance in ancient vertebrates. Recently, CD80/86 and CD83-like molecule were identified in several fish species, which provides molecular clues for the functional evaluation of these costimulatory molecules in the initial activation of adaptive immunity in fish (17–24). Given fish is the taxa of adaptive immunity origin and an evolutionary connection between primitive vertebrates and higher vertebrates (25), this study assessed the involvement of CD80/86 and CD83 in fish adaptive immunity to provide an understanding of the origin and evolution of the costimulatory mechanisms underlying adaptive immunity. Together with the exploration of B cells acting as initiating APCs in priming fish adaptive immunity, this study provides an across-species perspective on the evolutionary involvement of both costimulatory family members and B cell subsets as a whole.

Materials and Methods

Experimental fish

Zebrafish (*Danio rerio*) of both sexes, 3–12 mo of age and ~3–4 cm in body length, were raised in a circulating water bath at 28°C under standard laboratory conditions. All fish used in the experiments were offspring of a single AB strain parent pair after five generations of partial inbreeding (26, 27). Only healthy fish, as determined by general appearance and level of activity, were used for the study.

Bacterial strain

Vibrio alginolyticus (ATCC 17749) was cultured in trypticase soy broth medium (Life Technologies) on agar plates. Bacteria in exponential phase were collected for CFU assay and then heat inactivated at 65°C for 1 h. After washing, the bacterial suspensions were stored as aliquots at −80°C for use as the particulate Ag. For FITC conjugation, heat-inactivated *V. alginolyticus* (1×10^7 CFU) cells were labeled with FITC (0.2 mg/ml; Sigma-Aldrich) in 0.1 M carbonate buffer (pH 9) for 2 h, washed four times with PBS to remove unbound FITC, and adjusted to the appropriate concentrations (28).

Molecular cloning

Zebrafish CD80/86 and CD83 genes initially were predicted on the genomic and Expressed Sequence Tag databases maintained by the National Center for Biotechnology Information, University of California, Santa Cruz Genome Browser, Ensembl, TIGR Gene Indices, and FGENESH using Genscan and BLAST software programs, with mammalian CD80/86 and CD83 sequences as queries. CD80/86 and CD83 cDNA fragments were generated by RT-PCR. The primers used for this experiment are shown in Supplemental Table I. Total RNA was isolated from whole fish using TRIzol reagent (Invitrogen), treated with RNase-free DNase I (QIAGEN), and reverse transcribed into first-strand cDNA using an RNA PCR kit, according to the manufacturer's instructions (AMV version 3.0; TaKaRa). The 5′- and 3′-Full RACE Core Sets (TaKaRa) were used to obtain 5′− and 3′-unknown regions. PCR products were purified by a Gel Extraction Kit (QIAGEN), ligated into the pUCm-T vector (TaKaRa), and transformed into *Escherichia coli* Top10-competent cells (Invitrogen). Plasmid DNA was extracted by a Miniprep protocol (QIAGEN) and sequenced on a MegaBACE 1000 sequencer (GE Healthcare) using a DYEnamic ET dye terminator cycle sequencing kit (Pharmacia). Full-length cDNA fragments were assembled by catabolite gene activator protein (CAP 3.0).

Bioinformatics analysis

MapViewer and University of California, Santa Cruz Genome Browser were used to determine the comparative gene map positions of zebrafish CD80/86 and CD83. Gene organizations (intron/exon boundaries) were elucidated by comparing CD80/86 and CD83 cDNA fragments with genome sequences, and gene structures were drawn by GeneMapper 2.5. Putative signal peptides, transmembrane helices, and functional domains in zebrafish CD80/86 and CD83 proteins were predicted by SignalP 4.0 server, TMHMM 2.0 server, and PROSITE database (29). Amino acid sequence identity was calculated by MEGALIGN program from DNASTAR, and a multiple alignment was generated using the Clustal X program (version 1.81) (30). A neighbor-joining phylogenetic tree was constructed from pairwise Poisson correction distances, with 2000 bootstrap replications, using MEGA 4.1 software.

Real-time PCR

The expression patterns of CD80/86 and CD83 in various tissues, including kidney, spleen, liver, intestine, heart, gill, brain, skin, and muscle, and the upregulation of Lck and CD154 in activated T cells were quantified by real-time PCR on a Mastercycler ep realplex machine (Eppendorf, Hamburg, Germany) using a SYBR Premix Ex Taq kit (TaKaRa). Total RNA was extracted from tissues or cells using TRIzol reagent, measured by analysis on a 1.5% (w/v) agarose gel, and reverse transcribed into cDNA, as described above. All PCR reactions were performed in a total volume of 10 μl. PCR program was 94°C for 2 min, followed by 40 cycles at 94°C for 20 s, 55°C for 20 s, and 68°C for 20 s. Relative gene-expression level was calculated by the $2^{-\Delta\Delta CT}$ method normalized to β-actin. The primers used for this experiment are shown in Supplemental Table I. In all cases, each sample was run in triplicate parallel reactions. The experiments were repeated independently at least three times.

Production of recombinant proteins

Recombinant proteins of zebrafish CD80/86, CD83, and CD4 were prepared as previously described (31–34). Briefly, sequences encoding these proteins were amplified with primers (Supplemental Table I) containing corresponding restriction sites at the 5′- and the 3′-ends. The resulting PCR products were digested and subcloned into pET28a. Single colonies of *E. coli* Rosetta (DE3) pLysS harboring the expression plasmids were inoculated into Luria–Bertani medium (100 ml) containing chloramphenicol (100 mg/l) and kanamycin (25 mg/l). The colonies were then incubated with shaking at 37°C until an OD_{600} value of 0.6 was reached. Subsequently, isopropylthio-β-galactoside was added to a final concentration of 1 mM. The cultures were continued for 6 h. The expression levels of the proteins were assessed by 12% SDS-PAGE gel, followed by Coomassie Brilliant Blue R250 staining. The recombinant proteins were purified using Ni-NTA agarose affinity chromatography, according to the manual of QIA expressionist (QIAGEN).

Preparation of polyclonal Abs

Six-week-old male New Zealand white rabbits and BALB/c mice were immunized eight times at biweekly intervals with 20–100 μg purified recombinant proteins (CD80/86, CD83, and CD4) in CFA. One week after the final immunization, rabbits and mice were bled when Ab titers were > 1:10,000, as determined by microplate-based ELISA using recombinant proteins adsorbed to the solid phase. The Abs were affinity purified into IgG isotype by a protein A agarose column (QIAGEN) and purified further using an immunosorbent-based protocol, as previously described (35). The titers and specificities of the Abs were assessed by Ag-specific ELISA and Western blot, as previously described (Supplemental Fig. 1) (35). The purified polyclonal Abs against MHC class II, IgM, and CD154 were prepared and assessed for specificities in previous studies (31, 32).

Cell preparation and sorting

The blood, spleens, and head kidneys (HKs) from 30 fish were collected in ice-cold Ca^{2+}/Mg^{2+}-free HBSS with heparin (10 U/ml). Whole-blood cell suspensions were obtained with heparinized capillary tubes, and single-cell suspensions of spleens and HKs were prepared by gently teasing the tissues through an 80-μm nylon mesh filter. Lymphocytes were enriched from the cell suspensions by Ficoll-Hypaque (1.080 g/ml) centrifugation at 2500 rpm for 25 min at room temperature, collected from the interface layer, and washed with ice-cold Ca^{2+}/Mg^{2+}-free HBSS. Cellular viability was determined by trypan blue (0.4%) exclusion assay. For membrane IgM $(mIgm)^+$ B and $CD4^+$ T cell separation, immunomagnetic sorting (MACS) was performed, as previously described (33). Briefly, lymphocytes were adjusted to ~2×10^8 cells/ml. After blocking with 5% normal goat serum for 15 min at 10°C, the cell suspension was incubated with rabbit anti-mIgM or mouse anti-CD4 Ab for 15 min at 10°C, washed with MACS buffer (PBS containing 2 mM EDTA and 0.5% BSA), and incubated for 15 min at 10°C with anti-rabbit or anti-mouse IgG magnetic beads (Miltenyi Biotec). The cell suspension was applied to an LS separation column,

according to the manufacturer's instructions. The positive cells were cultured in L-15 medium (Life Technologies) supplemented with 10% FBS (Life Technologies), 1% L-glutamine, 1.5% HEPES, 100 U/ml penicillin, and 100 μg/ml streptomycin at 28°C overnight to detach the magnetic beads. The purity of the sorted mIgM$^+$ B and CD4$^+$ T cells was determined by flow cytometry, Wright-Giemsa staining, and RT-PCR. The primary Abs with the opposite source, mouse anti-mIgM and rabbit anti-CD4, were used for flow cytometry. Markers for B cells (mIgM and MHC class II), CD4$^+$ T cells (CD4, TCRα, and TCRβ), myeloid cells (CSF-1R, FcεRIγ, and mpeg1), eosinophils (Gata2), neutrophils (mpx), mast cells (cpa5), and erythrocytes (Gata1) were examined by RT-PCR.

Flow cytometric analysis

Cell suspensions were blocked with 5% normal goat serum for 1 h at 4°C and then incubated with corresponding primary Abs or normal mouse/rabbit IgG as isotype control for 1 h at 4°C. After washing, the samples were incubated with secondary FITC/PE-conjugated anti-rabbit/mouse IgG (Chemicon) for 1 h at 4°C. After washing, the fluorescence signals were determined immediately by a FACScan flow cytometer (BD Biosciences) equipped with an argon laser with emission at 488 nm. At least 10,000 events were collected from the lymphocyte gate (36). CellQuest software (BD Biosciences) was used for flow cytometric analyses, and ModFit LT software was used for T cell proliferation assays.

Evaluation of phagocytosis

Phagocytosis of mIgM$^+$ B cells was determined by an in vitro phagocytic assay. For this, 0.1 mg FITC-conjugated keyhole limpet hemocyanin (KLH) (FITC-KLH; Sigma-Aldrich) or 2×10^7 FITC-conjugated *V. alginolyticus* (FITC-V.A.) was added to 2×10^6 sorted mIgM$^+$ B cells in a 96-well plate and then incubated with B cells under different conditions, including for 3 h at 4°C (group 0 h); 1 h at 28°C, followed by 2 h at 4°C (group 1 h); 2 h at 28°C, followed by 1 h at 4°C (group 2 h); and 3 h at 28°C (group 3 h). After washing, the nonphagocytized membrane-bound FITC signals were quenched by 0.2% trypan blue for 5 min at 4°C (4, 37). In parallel, B cells incubated with FITC-KLH or FITC-V.A. at 28°C for 3 h in the presence of cytochalasin B (0.08 mg/ml; Sigma-Aldrich) were set as controls. Subsequently, the cells were washed and stained with mouse anti-mIgM and PE-conjugated anti-mouse IgG for flow cytometric analysis.

In vitro Ag-presentation assay

At 5 d before sacrifice, fish were immunized by i.p. injection with 10 μg KLH (Sigma-Aldrich; in combination with 10 ng LPS from *E. coli* serotypes O55:B5; Sigma-Aldrich) or *V. alginolyticus* (2×10^7 CFU/fish). Subsequently, Ag-stimulated CD4$^+$ T cells, including KLH-stimulated CD4$^+$ T cells (CD4$^+$ T_{KLH}) and *V. alginolyticus*–stimulated CD4$^+$ T cells (CD4$^+$ $T_{V.A.}$) were magnetically sorted from blood, spleens, and HKs and stained with 5 μM CFSE (Beyotime) for 8 min at room temperature. After the reactions were terminated by supplementing with 10% FBS (in L-15 medium), the cells were washed three times with this medium. Meanwhile, primary mIgM$^+$ B cells were magnetically isolated from untreated fish, incubated with Ags in different combinations, including 10 μg KLH, 100 ng LPS, 10 μg KLH plus 100 ng LPS, and 2×10^7 CFU *V. alginolyticus* for 8 h, and washed three times to eliminate noningested Ags. For Ag-presentation–inhibition assays, B cells were treated with chloroquine (80 μM; Sigma-Aldrich) for 1 h and then incubated with Ags in the presence of 80 μM chloroquine (38). These in vitro Ag-loaded B cells were cocultured with CFSE-labeled CD4$^+$ T_{KLH} and CD4$^+$ $T_{V.A.}$ cells in 96-well plates (Corning) at concentrations of 2×10^6 cells/well to 1×10^6 cells/well. Cyclosporin A (CsA; Sigma-Aldrich, 0.1 μg/ml) was used in the experiments as a T cell inhibitor control. The KLH plus LPS-pulsed and *V. alginolyticus*–pulsed B cells were cocultured with CFSE-labeled CD4$^+$ $T_{V.A.}$ and CD4$^+$ T_{KLH} cells, respectively, in the cross-stimulation control groups. After 3 d of coculture, the cells were labeled with primary mouse anti-CD4 Ab and secondary PE-conjugated anti-mouse IgG Ab. Proliferation of T cells was examined by flow cytometry through detecting the division of CFSE-labeled cells in PE-CD4$^+$ cell gate. The activation of T cells was determined as the upregulation of Lck and CD154 by real-time PCR. The primers used for this experiment are shown in Supplemental Table I.

In vivo B cell–presentation–blockade assay

Fish were injected i.p. three times with rabbit anti-mIgM or nonspecific rabbit IgG (as control) at a dose of 10 μg/fish, followed by administration of Ags (10 μg KLH plus 10 ng LPS or 2×10^7 CFU *V. alginolyticus*), as previously described (33, 39). In parallel, the PBS-treated group was set as a negative control. At 3 d after the last Ag stimulation and Ab administration, deletion of mIgM$^+$ B cells was examined by flow cytometric analysis and real-time PCR. In addition, proliferation/activation of Ag-

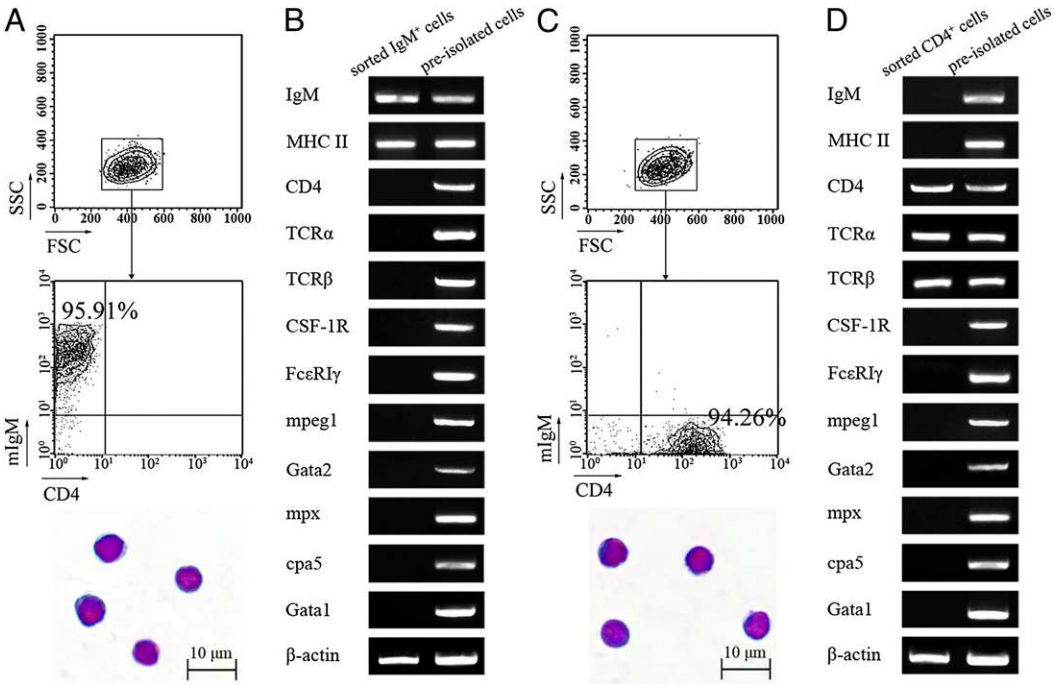

FIGURE 1. Assessment of the purity of magnetically sorted mIgM$^+$ B cells (**A**, **B**) and CD4$^+$ T cells (**C**, **D**). The number in each quadrant indicates the percentage of mIgM$^+$CD4$^-$ B cells (A) and mIgM$^-$CD4$^+$ T cells (C), respectively. Wright-Giemsa staining indicates the morphology of the sorted B cells (A) and T cells (C). Original magnification ×1000. (B and D) RT-PCR assay analyzed the expression of mIgM$^+$ B cell markers (IgM and MHC II), CD4$^+$ T cell markers (CD4, TCRα, and TCRβ), myeloid cell (monocyte/macrophage and DC) markers (CSF-1R, FcεRIγ, and mpeg1), eosinophil marker (Gata2), neutrophil marker (mpx), mast cell marker (cpa5), and erythrocyte marker (Gata1) in sorted mIgM$^+$ B cells (B) and CD4$^+$ T cells (D). The expression of these markers from preisolated cells without Ficoll-Hypaque isolation and magnetic sorting were used as positive control.

specific T cells was evaluated from the expression of Lck and CD154 in PBLs or head kidney lymphocytes (HKLs) by real-time PCR. The percentage of $CD4^+CD154^+$ T cells in lymphocytes from the blood, spleens, and HKs was determined using mouse anti-CD4 and rabbit anti-CD154 as primary Abs and FITC-conjugated anti-rabbit IgG and PE-conjugated anti-mouse IgG as secondary Abs for flow cytometry.

Adoptive-transfer assay

$mIgM^+$ B cells were sorted from unstimulated fish and then exposed to 10 μg KLH (in combination with 100 ng LPS) or 2×10^7 *V. alginolyticus* for 8 h. Subsequently, the cells were washed three times with culture medium to eliminate the free Ags, adjusted to 1×10^5 cells/μl, and injected i.p. into unstimulated recipient fish with 10 μl cell suspensions. After 3 d, lymphocytes were isolated from the recipient fish. T cell proliferation and activation were determined from the percentage of $CD4^+CD154^+$ T cells and the expression of Lck and CD154 molecules by flow cytometric analysis and real-time PCR, following the procedures described above.

Expression analysis of CD80/86 and CD83 on B cells

Expression of CD80/86 and CD83 on $mIgM^+$ B cells in response to Ag stimulation was examined both in vivo and in vitro. For in vivo assay, fish were stimulated with KLH in different combinations (10 μg KLH, 10 ng LPS, and 10 μg KLH plus 10 ng LPS) for 72 h. Then, $mIgM^+$ B cells were magnetically sorted from blood, spleens, and HK cell suspensions. The cells were incubated with primary Abs (rabbit anti-CD80/86 or anti-CD83, mouse anti-mIgM) and then with secondary Abs (FITC-conjugated anti-rabbit IgG and PE-conjugated anti-mouse IgG) for flow cytometric analyses. CD80/86 and CD83 also were examined in sorted B cells by real-time PCR. The primers used for this experiment are shown in Supplemental Table I. For in vitro assay, primary $mIgM^+$ B cells were sorted from untreated fish and then stimulated with KLH in different combinations (10 μg KLH, 100 ng LPS, and 10 μg KLH plus 100 ng LPS). After 8 h of incubation, the cells were harvested, and the expression levels of CD80/86 and CD83 were examined by flow cytometry and real-time PCR.

Immunofluorescence staining

At 3 d post-i.p. injection with 10 μg KLH and 10 ng LPS, lymphocytes were collected from the blood, spleens, and HKs and fixed with 2% paraformaldehyde fixative for 10 min at room temperature. Subsequently, the cells were blocked with 5% normal goat serum and then incubated with primary Abs (mouse anti-mIgM, along with rabbit anti-MHC class II, rabbit anti-CD80/86, or rabbit anti-CD83) at 4°C for 1 h. In parallel, the nonrelated Abs rabbit IgG and mouse IgG were used as negative controls. After washing, the cells were incubated with secondary FITC- and PE-conjugated anti-rabbit and anti-mouse IgG at 4°C for 1 h. Additional staining with DAPI was performed before photomicrography. Fluorescence images of the samples were obtained by a two-photon laser-scanning microscope (Zeiss LSM710 NLO; Carl Zeiss, Oberkochen, Germany) at ×630 magnifications.

Screening of small interfering RNAs against CD80/86 and CD83

The small interfering RNAs (siRNAs) against CD80/86 and CD83 were predicted by BLOCK-iT RNAi Designer (Invitrogen) and siDESIGN Center (Thermo Scientific). Three pairs of segments of each molecule were screened from >50 candidates. Short hairpin RNAs containing the selected siRNA sequences, as well as the nonrelated scrambled siRNA, were designed (Supplemental Table I). DNA oligonucleotides for short hairpin RNA expression (termed CD80/86 siRNA-1–3 and CD83 siRNA-1–3) were synthesized by Invitrogen, annealed, and constructed into pSUPER vector (pSUPER.retro.puro; Oligoengine, Seattle, WA) downstream of the

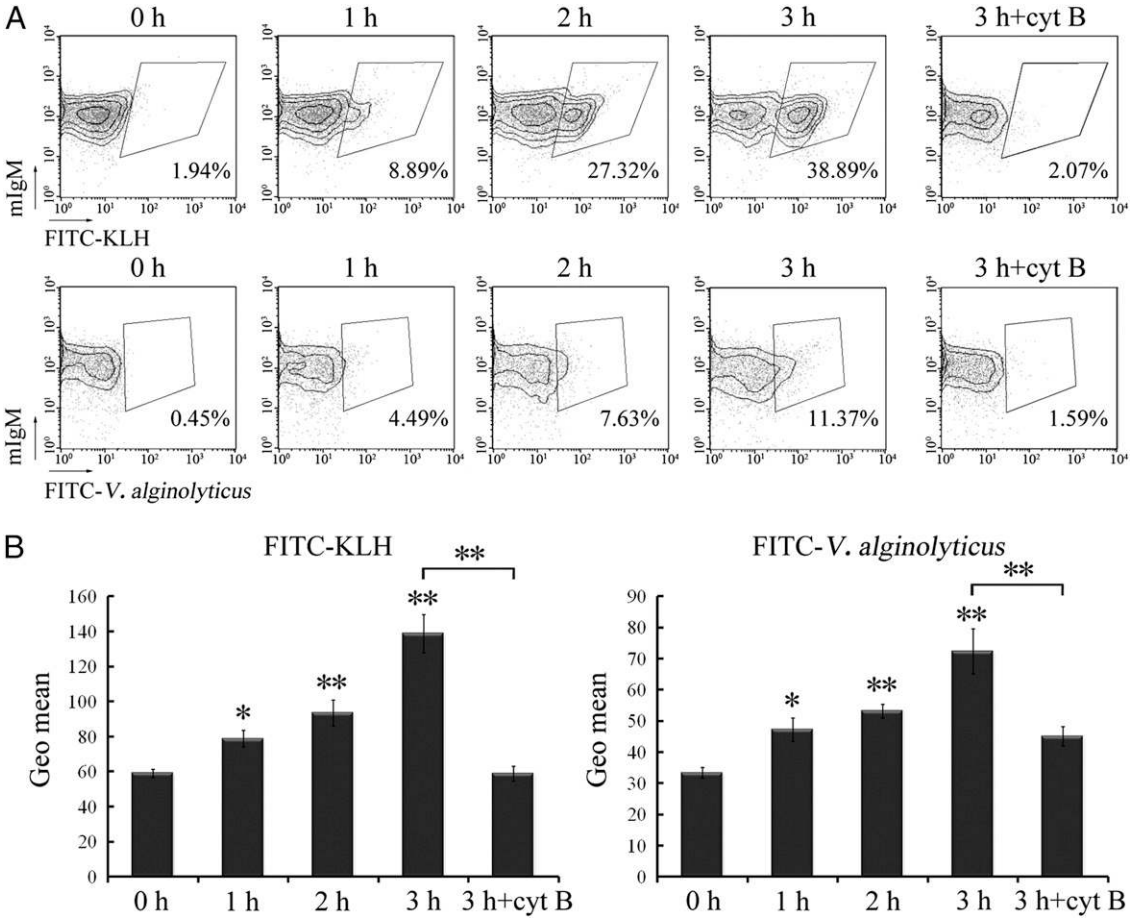

FIGURE 2. Phagocytic ability of zebrafish B cells. (**A**) $mIgM^+$ B cells were magnetically sorted and incubated with FITC-KLH or FITC-V.A. at 28°C for various periods. B cells incubated with either of these two Ags at 28°C for 3 h in the presence of cytochalasin B were set as control. The numbers under the outlined area in each panel indicate the percentages of phagocytic $mIgM^+$ B cells. (**B**) The geometric means of the green fluorescence intensities computed from the outlined gate represent the phagocytic ability of $mIgM^+$ B cells in each treatment group. Error bars represent SE. Data are from three independent experiments for each panel. $*p < 0.05$, $**p < 0.01$.

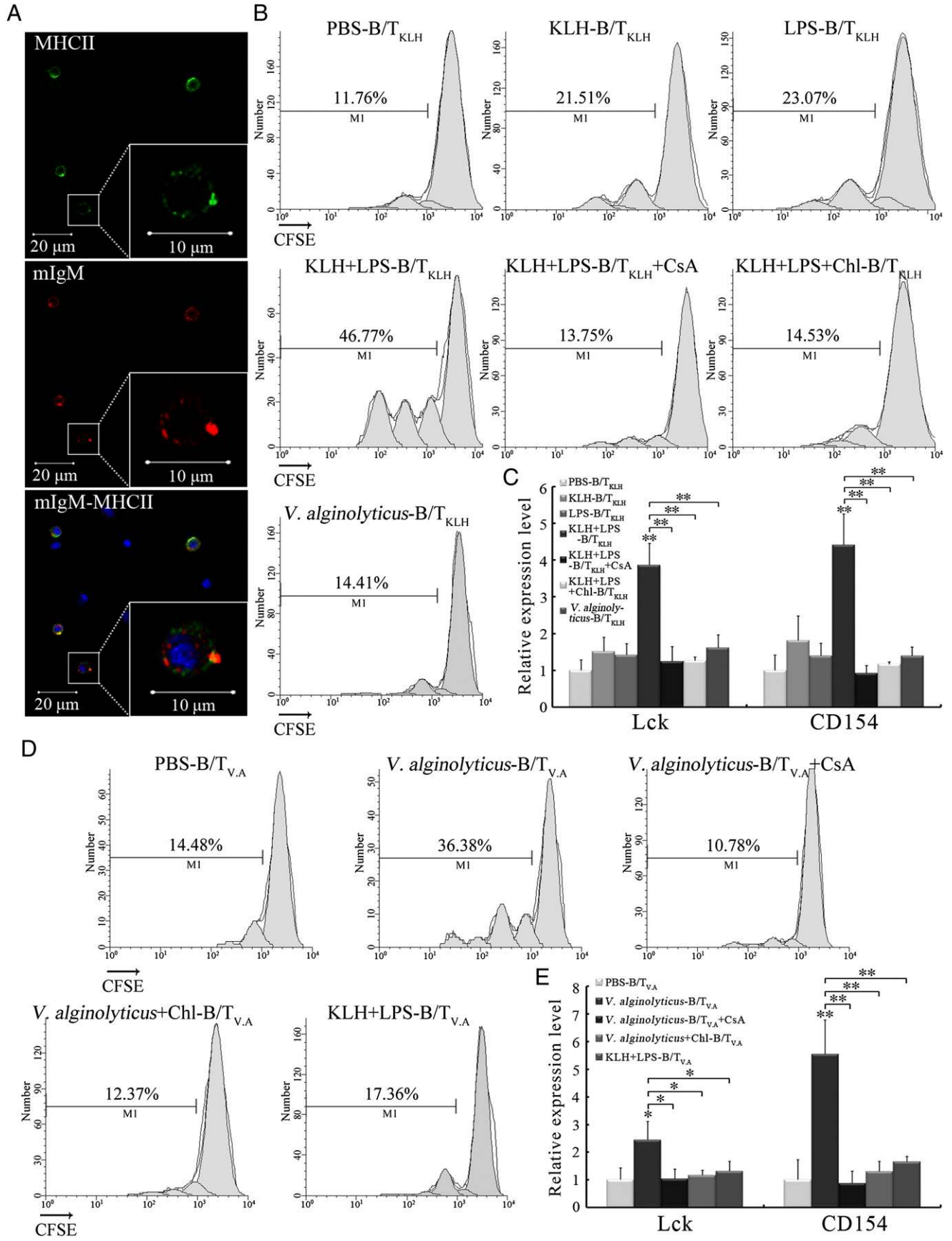

FIGURE 3. In vitro determination of Ag-presenting capacity of zebrafish B cells. (**A**) Immunofluorescence staining of mIgM$^+$MHCII$^+$ cells. Lymphocytes were stained with mouse anti-mIgM and rabbit anti–MHC II. Nonrelated Abs, including mouse IgG and rabbit IgG, were used as negative controls (data not shown). DAPI stain showed the location of the nuclei. The images were obtained using a two-photon laser-scanning microscope. Original magnification ×630. A T cell–proliferation assay was conducted to analyze the Ag-presenting ability of primary mIgM$^+$ B cells (*Figure legend continues*)

H1 promoter, as previously described (40, 41). The generated constructs with different siRNAs (2 μg) or control pSUPER (2 μg) along with overexpression plasmid (pcDNA6-CD80/86 or pcDNA6-CD83; 2 μg) were cotransfected into HEK293T cells. The efficiency of siRNAs against CD80/86 or CD83 was determined by real-time PCR.

Production of siRNA-encoding lentiviruses

The U6 promoter cassette in lentiviral vector pLB was replaced by the H1-siRNA cassette excised from the most effective siRNA constructs (pSUPER-CD80/86siRNA-1 and pSUPER-CD83siRNA-3) to produce pLB-CD80/86 and pLB-CD83 lentiviral vectors. Lentiviruses (LVs) were generated using packaging HEK293T cell line, according to standard protocols (40, 41). Briefly, LV vectors (20 μg) were cotransfected with pCMV-dR8.2 dvpr (15 μg) and pCMV-VSVG (6 μg) packaging vectors into HEK293T cells using Lipofectamine 2000 (Invitrogen). The LV supernatant was harvested at 48–72 h posttransfection, concentrated via ultracentrifugation at 25,000 rpm for 90 min at 4°C (SW-41Ti rotor), and dissolved in PBS. Because the pLB plasmid contains a GFP expression gene operated by the CMV promoter, the viral titers were determined by transduction and flow cytometric analysis of GFP expression in HEK293T cells. Infected cells were examined under a fluorescent microscope (Zeiss Axiovert 40 CFL; Carl Zeiss, Oberkochen, Germany).

Efficiency of LVs

The silencing efficiency of the constructed LVs was determined both in vitro and in vivo. For in vitro detection, HEK293T cells were transfected with pcDNA6-CD80/86 or pcDNA6-CD83. At 24 h posttransfection, 10 μl concentrated LV was added to the culture medium, and the expression level of CD80/86 or CD83 was determined by real-time PCR. For in vivo assay, the LV (2×10^5 TU/ml) was repeatedly delivered into fish by i.p injection once a day for 3 d. In parallel, the control group was injected with scrambled siRNA-harboring LV. Total RNA from PBLs and HKLs was isolated and reversed transcribed into cDNA. Real-time PCR was conducted to evaluate the efficiency of in vivo knockdown of CD80/86 or CD83.

Role of CD80/86 and CD83 in T cell activation

The effects of CD80/86 and CD83 in T cell activation were examined by in vivo knockdown and blockade assays. For knockdown assays, fish were given LVs (scrambled siRNA-LV as control) three times, with 24-h time intervals. At the last administration, fish were coinjected with KLH (10 μg; in combination with 10 ng LPS/fish). For blockade assays, fish were injected i.p. with KLH (10 μg; in combination with 10 ng LPS/fish), followed by three administrations of rabbit anti-CD80/86 or anti-CD83 Ab (10 μg/fish each time; nonspecific rabbit IgG as control). Lymphocytes were isolated from the blood, spleen, and HK tissues 3 d after Ag stimulation. The proliferation and activation of $CD4^+$ T cells were assessed by flow cytometry and real-time PCR.

Role of CD80/86 and CD83 in B cell–initiated T cell activation

The magnetically sorted primary $mIgM^+$ B cells were stimulated with KLH, and the Ag-primed $CD4^+$ T cells were labeled with CFSE, as described above. Then, they were cocultured for 72 h. During this period, rabbit anti-CD80/86 (5 μg/ml), rabbit anti-CD83 (5 μg/ml), or control rabbit IgG (5 μg/ml) was added to the cells every 24 h. The proliferation and activation of $CD4^+$ T cells were examined by flow cytometry and real-time PCR.

Statistical analysis

Statistical evaluation of differences between means of experimental groups was done using ANOVA and multiple Student tests. Both $p < 0.05$ and $p < 0.01$ were considered statistically significant. The sample number for each group was >10 fish. Data points represent the means of three independent experiments.

Results

Phagocytic capacity of zebrafish B cells

The phagocytic capacity of teleost B cells has been well studied in several fish species, suggesting that phagocytosis might be a common feature of teleost B cells (4, 5, 42). As additional support, the phagocytic capacity of zebrafish B cells was examined by flow cytometry, which is also a prelude for the determination of B cells in zebrafish acting as a kind of initiating APC. $mIgM^+$ B cells were magnetically sorted from the selected tissues and examined to share a high degree of purity > 95%. Sorted cells were scarcely detected outside of the forward/side scatter–based lymphocyte gate by flow cytometry (Fig. 1A). They showed typical lymphocyte morphology and expressed B cell hallmarks (mIgM and MHC class II) but not T cell markers (CD4, TCRα, TCRβ), myeloid cell (monocyte/macrophage and DC) markers (CSF-1R, FcεRIγ, mpeg1), eosinophil marker (Gata2), neutrophil marker (mpx), mast cell marker (cpa5), or erythrocyte marker (Gata-1) (Fig. 1B). When incubated with FITC-KLH or FITC-V.A. at 28°C, the percentages of phagocytic $mIgM^+$ B cells reached 38.89 ± 6.35% and 11.37 ± 1.59%, respectively, which were significantly higher than the 1.94 ± 0.33% for FITC-KLH and 0.45 ± 0.08% for FITC-V.A. in the control groups at 4°C. Meanwhile, cytochalasin B treatment greatly inhibit both FITC-KLH and FITC–V.A. uptake by $mIgM^+$ B cells, indicating an actin polymerization–dependent phagocytic ability of $mIgM^+$ B cells (Fig. 2A). Enhanced amounts of Ag phagocytosis by $mIgM^+$ B cells also were determined by the mean fluorescence intensity of FITC (Fig. 2B). As expected, these results indicate that zebrafish B cells have potent nonspecific phagocytic ability for both soluble and particulate Ags, which was consistent with previous reports for other fish, suggesting the existence of a universal phagocytic role that fish B cells possess during primitive vertebrate evolution.

In vitro determination of Ag-presenting capacity of zebrafish B cells

To explore whether zebrafish B cells can present both soluble and particulate Ags to $CD4^+$ T cells, an in vitro T cell–activation assay was performed. Earlier, the distribution of MHC class II, a specific APC marker for presenting Ags to $CD4^+$ T cells, was determined on the B cells to provide initial evidence that zebrafish B cells act as professional APCs. Double-immunofluorescence staining showed that a considerable number of lymphocytes generated from Ag (KLH)-stimulated fish exhibited high coexpression of MHC class II and mIgM (Fig. 3A). In contrast, lymphocytes from untreated fish showed low MHC class II expression on $mIgM^+$ B cells (data not shown). This result suggests that MHC class II was expressed on zebrafish B cells in an inducible manner, similar to that on mammals. For in vitro T cell–activation assay, the primary $mIgM^+$ B cells were sorted from unstimulated fish and boosted in vitro by

loaded with soluble (**B**) or particulate (**D**) Ags in vitro. B cells were incubated separately with KLH, LPS, or KLH plus LPS (B) or *V. alginolyticus* (D) for 8 h, followed by coculturing with CFSE-labeled $CD4^+$ T_{KLH} or $T_{V.A.}$ cells for 3 d. T cell proliferation induced by the mock PBS-loaded B cells was set as a blank control. CsA was added to the cocultured cell suspensions in the KLH+LPS-B/T_{KLH}+CsA and *V. alginolyticus*–B/$T_{V.A.}$+CsA groups. Treatment of B cells with chloroquine before and during Ag pulsing was performed to inhibit the Ag-presenting function of B cells. $CD4^+$ T_{KLH} and $T_{V.A.}$ cells cocultured with *V. alginolyticus*–loaded and KLH+LPS-loaded B cells, respectively, were performed in the cross-stimulation control groups. Subsequently, flow cytometry was conducted to show $CD4^+$ T cell proliferation. The numbers above the bracketed lines indicate the percentage of CFSE-diluted cells in each panel. Data represent three independent experiments. Real-time PCR analyses were conducted to determine the expression levels of T cell proliferation and activation markers, Lck and CD154, in 3 d cocultured $CD4^+$ T_{KLH} or $T_{V.A.}$ cells and $mIgM^+$ B cells pulsed with soluble (**C**) or particulate (**E**) Ags. Relative gene expression was calculated using the $2^{-\Delta\Delta CT}$ method, with initial normalization of genes against β-actin within each treatment group. The expression levels of each gene in the control groups were arbitrarily set to 1.0. The relative expression values were averaged from the data in three parallel reactions, and the results were obtained from at least three independent experiments. Error bars represent SE. $^*p < 0.05$, $^{**}p < 0.01$.

KLH in combination with LPS, a pathogen-associated molecular pattern expected to provide a costimulatory signal. In parallel, the $CD4^+$ T_{KLH} were sorted from fish administered KLH in vivo (Fig. 1C, 1D) and then cocultured with the KLH-loaded B cells. As expected, the KLH-loaded B cells dramatically increased the cognate $CD4^+$ T_{KLH} cell proliferation by >4-fold compared with the mock PBS-loaded B cell controls. Ag-presentation–inhibition and cross-stimulation assays were performed to evaluate the potential allogenic reactions in the experiment. The result showed that $CD4^+$ T cell responses could be greatly repressed by incubating KLH-pulsed B cells with chloroquine, an inhibitor of intracellular endosomal proteolysis. Meanwhile, *V. alginolyticus*–pulsed B cells

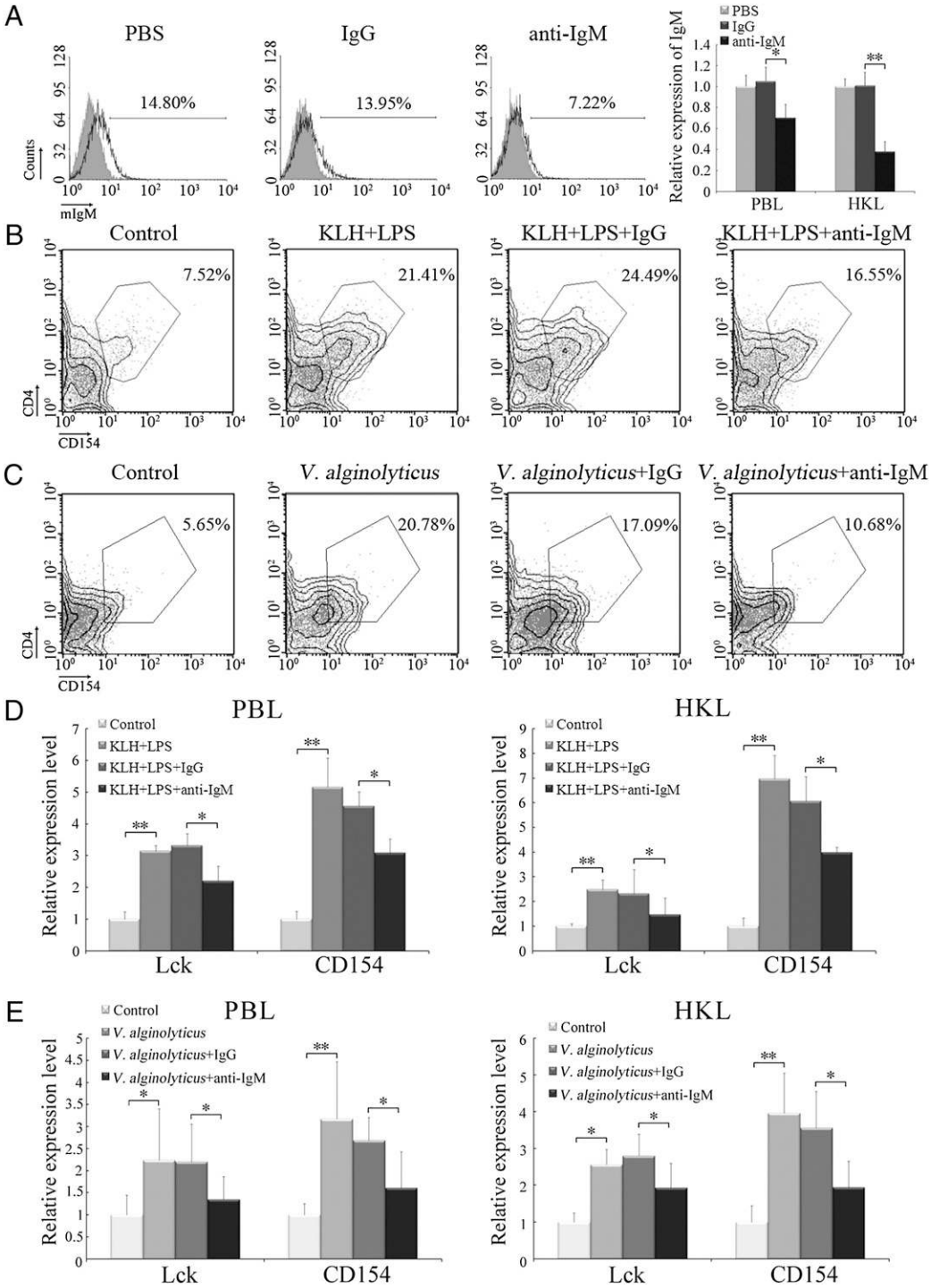

FIGURE 4. In vivo determination of Ag-presenting capacity of zebrafish B cells. (**A**) The effect of anti-mIgM Ab on in vivo depletion of $mIgM^+$ B cells was assessed by flow cytometry and real-time PCR. Negative controls treated with PBS or normal rabbit IgG were created. Shaded graphs show the background staining with an irrelevant Ab on the target gated population. The numbers above the bracketed lines indicate the percentage of $mIgM^+$ B cells in each treatment group. Error bars represent SE. Each result was obtained from 30 fish. The degree of $CD4^+$ T cell activation is represented by the percentage of $CD4^+CD154^+$ T cells determined by flow cytometry (**B**, **C**) and by the expression levels of Lck and CD154 detected by real-time PCR (**D**, **E**). In the flow cytometric analysis, different treatments are shown at the top of each block diagram. The numbers adjacent to the outlined areas indicate the percentages of $CD4^+CD154^+$ cells in each treatment group. In the real-time PCR assay, PCRs were run in combination with the endogenous β-actin control. Error bars represent SE. All data are from at least three independent experiments. $*p < 0.05$, $**p < 0.01$.

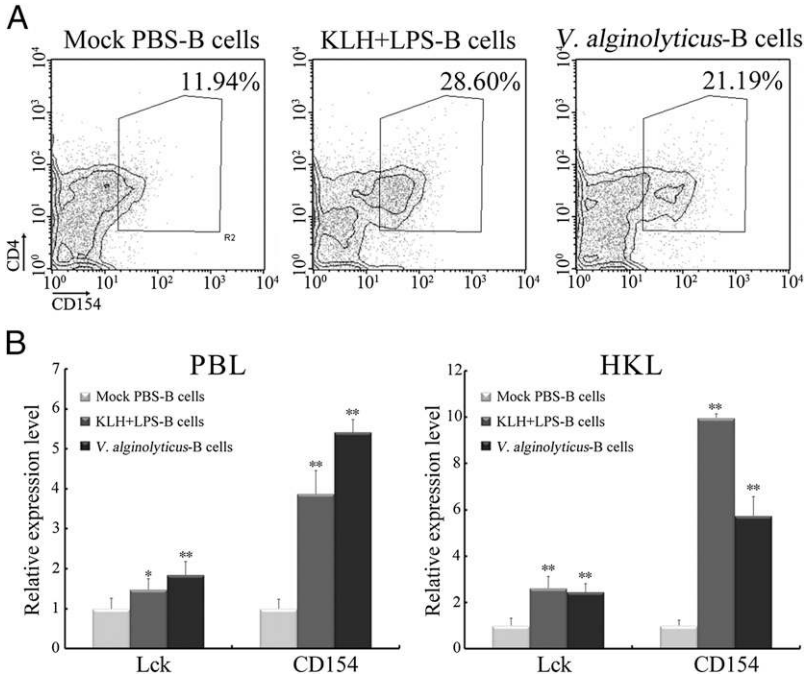

FIGURE 5. Ag-presenting capacity of zebrafish B cells to naive $CD4^+$ T cells. Primary $mIgM^+$ B cells were pulsed with PBS, KLH plus LPS, or *V. alginolyticus* for 8 h and injected i.p. into the recipient fish. After 3 d, the percentage of $CD4^+CD154^+$ T cells in the lymphocytes separated from blood, spleens, and HKs was measured by flow cytometry (**A**), and the expression levels of Lck and CD154 in PBLs and HKLs were determined by real-time PCR (**B**). Error bars represent SE. All data are from at least three independent experiments. $*p < 0.05$, $**p < 0.01$.

had considerably less effect on the increase in $CD4^+$ T_{KLH} proliferation compared with KLH-pulsed B cells (Fig. 3B). These results imply that the Ag-specific reaction is the major contributor to the increase in T cell proliferation. Meanwhile, the B cells loaded with KLH or LPS alone induced a lesser increase in $CD4^+$ T_{KLH} cell proliferation, suggesting that dual signals (Ag and costimulatory signals) are needed for priming Ag-specific $CD4^+$ T cell proliferation. In addition, the activation of $CD4^+$ T_{KLH} cells was determined by the expression of Lck and CD154, and a significant ($p < 0.01$) upregulation of T_{KLH} cells was detected in the coculture of B cells stimulated with KLH and LPS (Fig. 3C). Similar results were obtained when primary B cells were loaded with particulate Ags (*V. alginolyticus*) (Fig. 3D, 3E). These results clearly show that zebrafish B cells act as powerful presenting cells for both nonspecific soluble and particulate Ags to $CD4^+$ T cells.

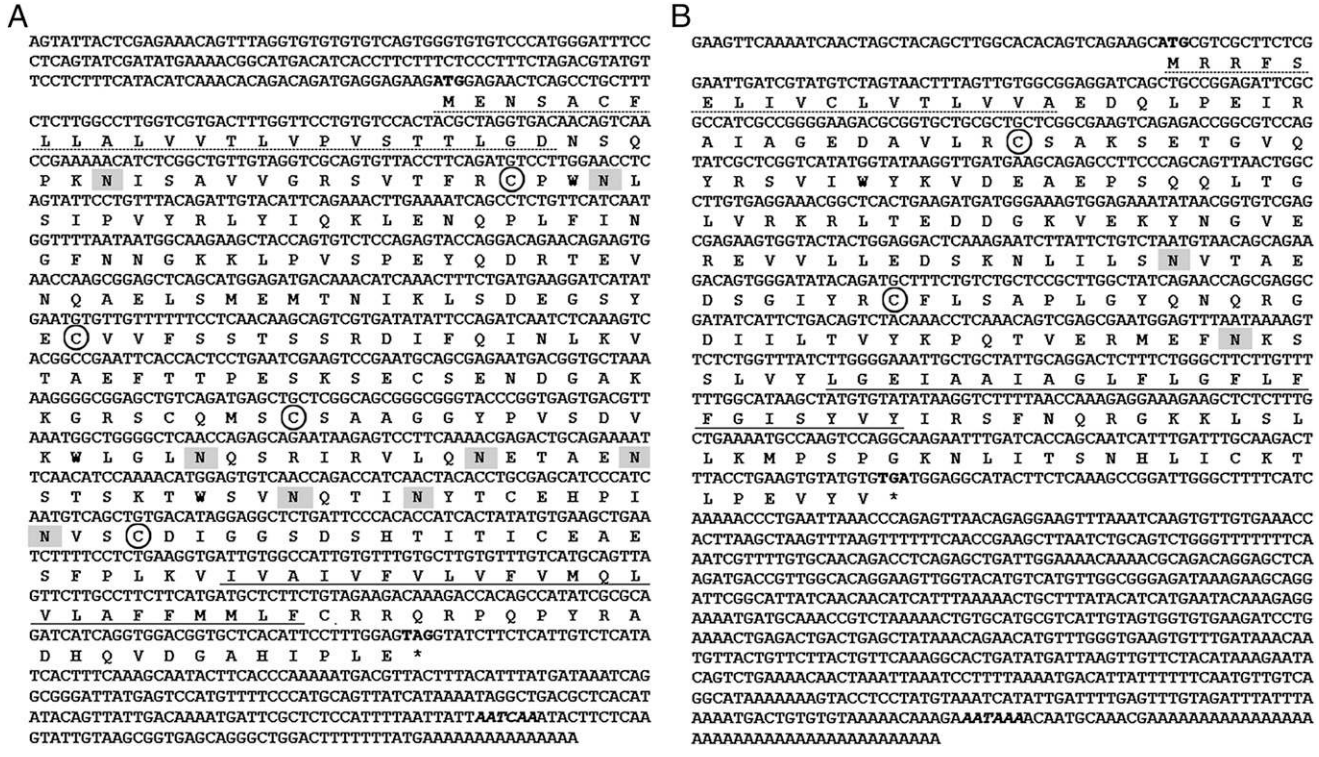

FIGURE 6. cDNA sequences and deduced amino acids of CD80/86 (**A**) and CD83 (**B**) from zebrafish. The start and stop codons are in bold type, and the putative polyadenylation signals are in bold italic type. The asterisks indicate peptide endings. Signal peptides and transmembrane hydrophobic regions are underlined. Four conserved cysteines in the CD80/86 nucleotide and two in the CD83 nucleotide forming Ig-like domain structures are circled. The locations of the predicted NGSs are shaded.

In vivo determination of Ag-presenting capacity of zebrafish B cells

To further clarify the involvement of zebrafish B cells in priming $CD4^+$ T cells, an in vivo–depletion assay was performed. Fish were administered anti-mIgM Ab; the amounts of $mIgM^+$ B cells were reduced by ~50% compared with the PBS- or nonrelated rabbit IgG–treated fish (Fig. 4A). The depletion effect was consistent with a previous study (33). Compared with the Ag-immunized normal groups, the proportion of activated T cells, upon administration of KLH (in combination with LPS) ($CD4^+CD154^+$ T_{KLH}) or *V. alginolyticus* ($CD4^+CD154^+$ $T_{V.A.}$), in the B cell–depleted groups decreased from 21.41 ± 3.17% to 16.55 ± 2.02% and from 20.78 ± 3.22% to 10.68 ± 1.96%, respectively. In contrast, no significant decrease in the percentages of $CD4^+CD154^+$ T_{KLH} (24.49 ± 2.99%) or $CD4^+CD154^+$ $T_{V.A}$ (17.09 ± 2.28%) was observed in the nonrelated IgG-treated groups compared with the normal immunized groups (Fig. 4B, 4C). Similarly, the expression levels of Lck and CD154 (upon KLH or *V. alginolyticus* stimulation) in PBLs and HKLs were dramatically ($p < 0.05$) downregulated in the B cell–depleted groups (Fig. 4D, 4E). These results provide in vivo evidence that zebrafish B cells are essential to initiate T cell activation in response to both soluble (KLH) and particulate (*V. alginolyticus*) Ags.

Ag-presenting capacity of zebrafish B cells to naive $CD4^+$ T cells

To further validate the role of B cells in priming naive $CD4^+$ T cells, adoptive transfer assays were performed. The sorted primary B cells were loaded in vitro with Ags and then transferred into unstimulated sibling recipient fish. After 3 d of transfer, the activation of the in vivo naive $CD4^+$ T cells was determined by their upregulation of CD4, CD154, and Lck markers. Flow cytometry showed that the percentages of activated $CD4^+$ T cells in response to KLH-loaded and *V. alginolyticus*–loaded B cells reached 28.60 ± 3.72% and 21.19 ± 2.54%, respectively, which were significantly ($p < 0.01$) higher than the basal level (11.94 ± 2.14%) in the mock PBS-treated B cell groups (Fig. 5A). Similarly, real-time PCR showed that CD154 and Lck in the PBLs and HKLs of recipient fish were significantly upregulated (Fig. 5B). These results strongly support the idea that zebrafish B cells are pivotal initiating APCs in priming naive $CD4^+$ T cells, a critical event in adaptive immunity.

Characterization of zebrafish CD80/86 and CD83

Full-length CD80/86 and CD83 cDNA fragments were identified in the zebrafish (GenBank accession numbers KC414844 and KC414845). CD80/86 cDNA was 1238 bp in length, comprising an 840-bp open reading frame encoding 279 aa. CD83 cDNA was

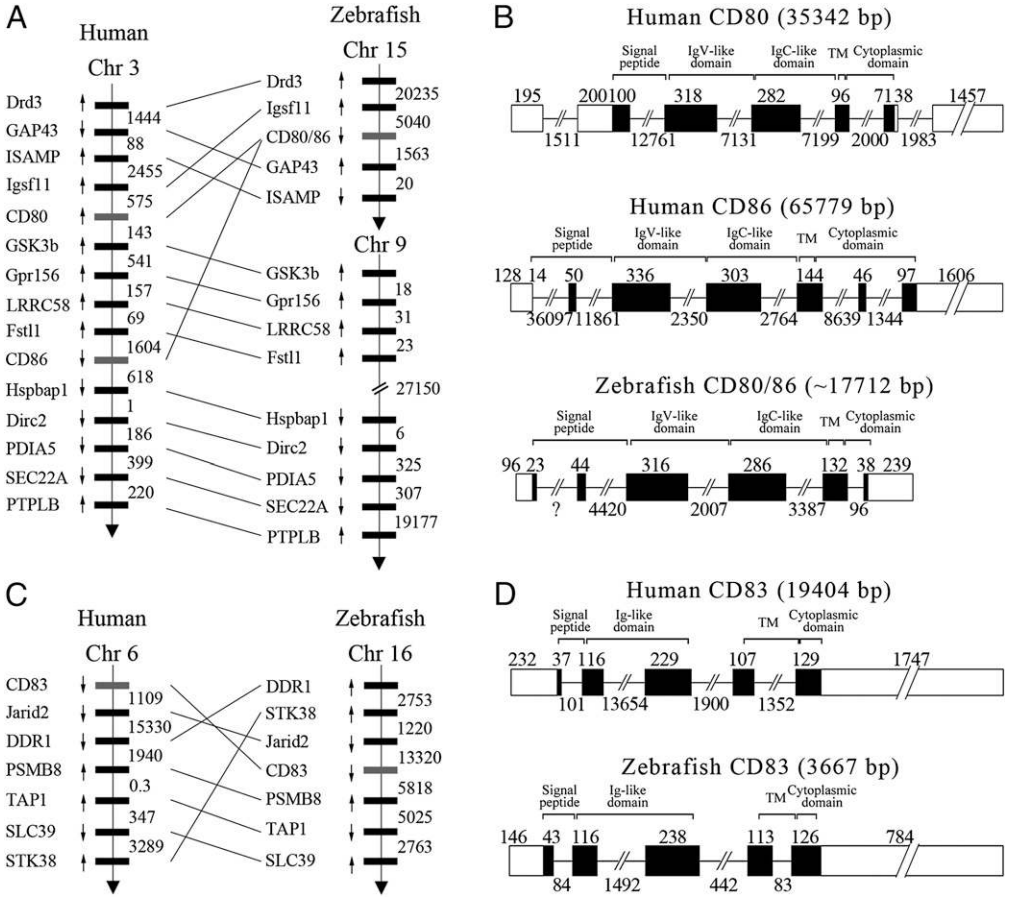

FIGURE 7. Comparative gene location and genomic structures of CD80/86 (**A**, **B**) and CD83 (**C**, **D**) between zebrafish and human. (A and C) Arrows indicate gene orientation. Numbers below gene blocks indicate the spacing (in kb) of adjacent genes. (B and D) The rectangles represent the exons, and the lines between them indicate the introns. Black and white areas indicate the coding regions and untranslated regions, respectively. The sizes of the exons and introns are shown by the numbers above and below, respectively, and the size of each whole gene (including exons and introns) is shown in parentheses after the gene name. The sequence encoding each domain is marked above the square bracket. The gene organization of CD80, CD86, and CD83 from human are derived from NM_005191.3 (human CD80), NM_175862.4 (human CD86), and NM_004233.3 (human CD83). ?, unknown size because of incomplete sequencing of the zebrafish genome.

1365 bp in length and included a 636-bp open reading frame encoding 211 aa (Fig. 6). The zebrafish CD80/86 and CD83 genes, located on chromosomes 15 and 16, spanned 17.7 and 3.67 kb and contained six and five exons, respectively, sharing overall conserved chromosome synteny and gene organization with their mammalian counterparts (Fig. 7). Notably, only a single CD80/86 gene exists in zebrafish, which is consistent with that found in other fish species (17, 18). The genes should be downstream, adjacent to the CD80/86 gene located on chromosome 9 instead of chromosome 15 (Fig. 7A). The organization of the zebrafish CD80/86 gene resembles that of the human CD86 gene, both in composition and in encoding sequences for functional domains. For example, the signal peptide, Ig V region-like (IgV-like), Ig C region-like (IgC-like), and transmembrane domains are encoded by exons 1–3, 3–4, 4–5, and inner 5 of both human CD86 and zebrafish CD80/86 genes, respectively. The zebrafish CD80/86 gene only differs from the human CD86 gene by its lack of exon 6, which is used to encode part of the cytoplasmic domain of human CD86. This difference suggests that the variation in signaling functions is associated with the evolution of CD86 from fish to mammals. In contrast, the genome organization of human CD80 is quite different from that of both the human CD86 and zebrafish CD80/86 genes (Fig. 7B). In parallel, the chromosome synteny and gene structures of CD83 genes seem highly conserved between zebrafish and human (Fig. 7C, 7D).

Structurally, zebrafish CD80/86 protein comprises an extracellular IgV-like domain (31–129) and an IgC-like domain (130–228), and CD83 protein contains a single Ig-like domain (21–130). Zebrafish CD80/86 and CD83 are type I transmembrane proteins with typical structural features of the Ig superfamily conserved throughout different organisms. Multiple alignments show that functional amino acid residues and Ig domains of zebrafish CD80/86 and CD83 share a high degree of homology with each molecule in higher vertebrates (Supplemental Figs. 2A, 3A). For instance, two pairs of Cys residues are engaged in two IgV and IgC loop structures of CD80/86, whereas one pair forms a single Ig-like domain of CD83, which are well conserved from fish to mammals. In addition, studies (43, 44) showed that mammalian CD80 and CD86 are highly glycosylated. Consistently, eight *N*-linked glycosylation sites (NGSs) can be predicted in zebrafish CD80/86, including one adjacent to the IgV-like domain, one inside the IgV-like domain, and six inside the IgC-like domain. This distribution of potential NGSs in zebrafish CD80/86 seems more conserved than that in mammalian CD86 (45, 46). Moreover, the extracellular domain of zebrafish CD83 contains two potential NGSs. The lack of the third potential NGS in mammals is consistent with other fish species. Phylogenetic analysis showed that both CD80/86 and CD83 are closely clustered with their homologs in different species, with high bootstrap probability (Supplemental Figs. 2B, 3B). These close genetic and structural relationships indicate the functional conservation of CD80/86 and CD83 homologs from fish to homeotherms during evolution.

Distribution of zebrafish CD80/86 and CD83

Tissue distribution analyses show that zebrafish CD80/86 and CD83 are ubiquitously expressed in various tissues, particularly in immune-relevant tissues, such as kidney, spleen, liver, and intestine (Fig. 8A). For functional evaluation of CD80/86 and CD83 in B cell–initiated immunity, their distributions on B cells were assessed. Results of the double-immunofluorescence staining indicated that CD80/86 and CD83 clearly colocalized with mIgM molecules (Fig. 8B). Furthermore, the expression levels of CD80/86 and CD83 in B cells were upregulated in response to Ag stimulation. After in vivo administration of KLH, LPS, or KLH plus LPS,

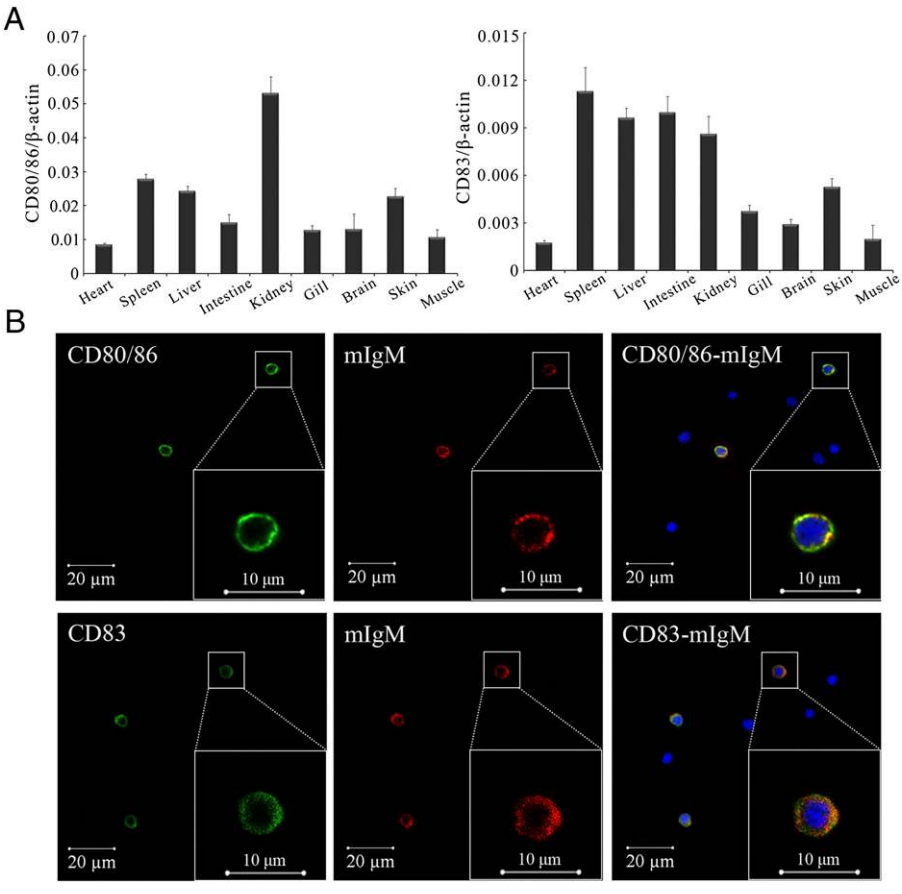

FIGURE 8. Distribution of zebrafish CD80/86 and CD83. (**A**) Relative gene-expression profiles of CD80/86 and CD83 in various adult fish tissues, as determined by real-time PCR, are displayed relative to the expression levels of β-actin (CD80/86/β-actin or CD83/β-actin). Each sample was obtained from 10 fish and run in triplicate parallel reactions. The experiments were repeated independently at least three times. (**B**) Immunofluorescence staining of lymphocytes separated from blood, spleens, and HKs of fish stimulated with KLH (in combination with LPS). Cells were stained with mouse anti-mIgM, together with rabbit anti-CD80/86 or rabbit anti-CD83. Nonrelated Abs, including mouse IgG and rabbit IgG, were used as negative controls (data not shown). DAPI stain shows the location of the nuclei. The images were obtained using a two-photon laser-scanning microscope. Original magnification ×630.

the percentages of mIgM$^+$CD80/86$^+$ and mIgM$^+$CD83$^+$ cells increased significantly in PBLs and HKLs compared with PBS-treated fish. Among the three stimulated groups, the one stimulated with KLH plus LPS had the most striking upregulation of mIgM$^+$CD80/86$^+$ and mIgM$^+$CD83$^+$ cells, which was higher than the sum of the KLH-alone and LPS-alone groups (Fig. 9A, 9B). The enhanced expression levels of CD80/86 and CD83 upon KLH and LPS stimulation also were detected in magnetically sorted mIgM$^+$ B cells by real-time PCR (Fig. 9C). Similarly, stimulating the sorted B cells with KLH, LPS, or KLH plus LPS in vitro increased the percentages of mIgM$^+$CD80/86$^+$ and mIgM$^+$CD83$^+$ cells and upregulated CD80/86 and CD83 in B cells, as determined using flow cytometry and real-time PCR (Fig. 9D–F). The finding that zebrafish CD80/86 and CD83 are distributed on B cells and can be upregulated upon Ag stimulation points to their possible roles in B cell–mediated adaptive immunity.

In vivo knockdown of CD80/86 and CD83

According to our previous study (40), the LV is a powerful delivery system for in vivo RNA interference knockdown in adult fish. Therefore, the LV delivery system was used in this study. Two siRNAs (CD80/86–siRNA-1 and CD83–siRNA-3) with the most effective (>80%) ability to separately induce CD80/86 and CD83 mRNA degradation were identified (Fig. 10A). These two siRNA-encoding sequences were introduced into LVs. Using a GFP-based detecting system and real-time PCR, the resulting viruses (CD80/86–siRNA-LV and CD83–siRNA-LV) showed strong infectious (>1 × 10^5 TU/μl) and interfering (>60%) abilities (Fig. 10B–D). After in vivo administration of three doses of CD80/86–siRNA-LV or CD83–siRNA-LV (i.p., 2 × 10^5 TU/fish) into zebrafish with 24-h time intervals, the expression levels of CD80/86 and CD83 were strongly inhibited (~70%) in PBLs and HKLs (Fig. 10E).

In vivo evaluation of CD80/86 and CD83 in CD4$^+$ T cell activation

In vivo knockdown and Ab-blockade assays were performed to evaluate the roles of CD80/86 and CD83 in CD4$^+$ T cell activation. Using flow cytometry, the administration of CD80/86–siRNA-LV, CD83–siRNA-LV, anti-CD80/86, and anti-CD83 dramatically inhibited CD4$^+$ T cell activation: the percentages of CD4$^+$CD154$^+$ T cells in Ag-stimulated lymphocytes from blood, spleen, and HKs decreased from 27.86 ± 3.01% (Ag plus scrambled siRNA-LV group) and 24.49 ± 2.13% (Ag plus IgG group) to 9.76 ± 1.57% (Ag plus CD80/86-siRNA-LV group), 10.14 ± 2.01% (Ag plus CD83-siRNA-LV group), 14.13 ± 2.21% (Ag plus anti-CD80/86 group), and 14.87 ± 1.88% (Ag plus anti-CD83 group), respectively (Fig. 11A). Similarly, the expression levels of Lck and CD154 in PBLs and HKLs decreased substantially after the knockdown and blockade of CD80/86 and CD83 molecules (Fig. 11B). These results suggest that both CD80/86 and CD83 are essential for the activation of CD4$^+$ T cells.

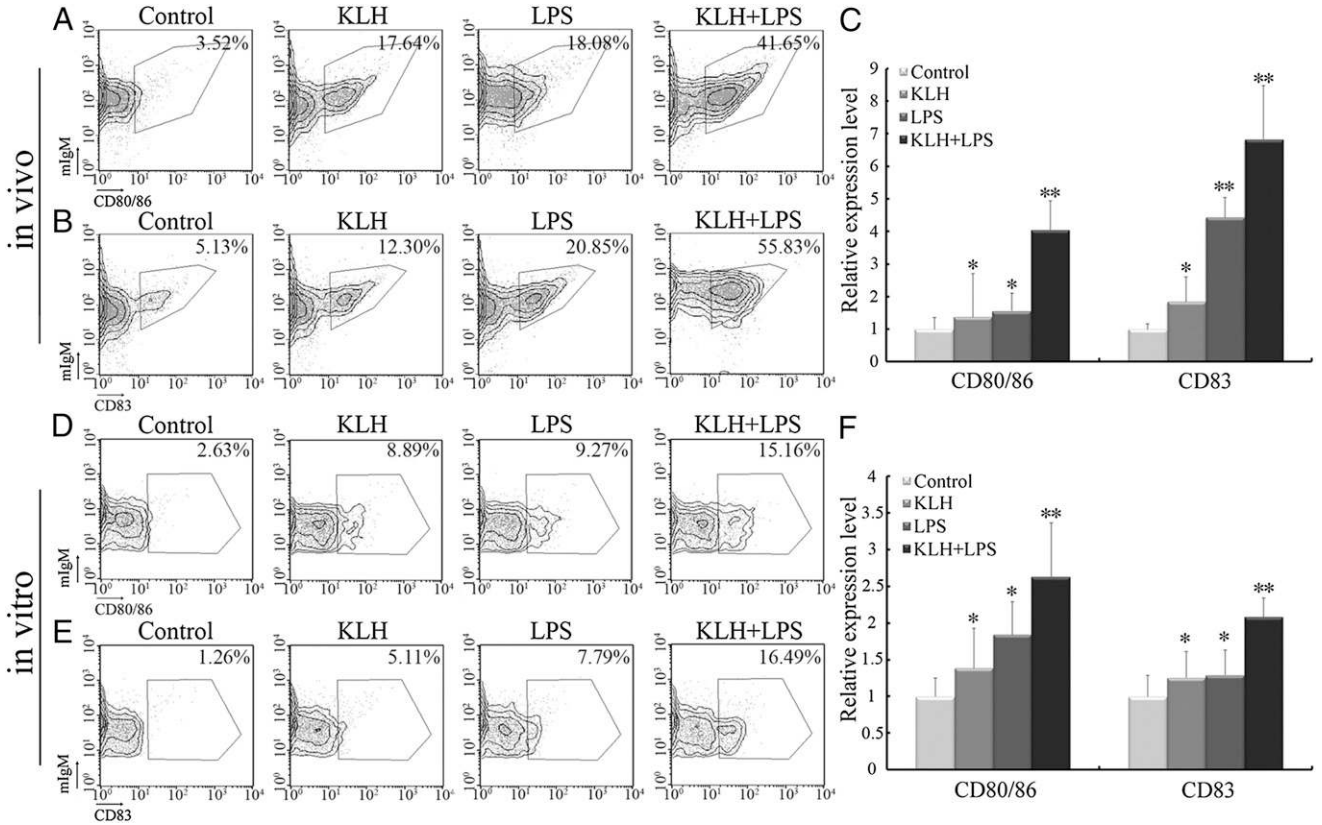

FIGURE 9. Upregulation of CD80/86 and CD83 expression on mIgM$^+$ B cells upon Ag stimulation. Flow cytometric analyses of CD80/86 (**A**) and CD83 (**B**) expression levels on mIgM$^+$ B cells, which were sorted from peripheral blood, spleens, and HKs 3 d after i.p. stimulation with PBS, KLH, LPS, or KLH plus LPS. The numbers above the outlined areas indicate the percentage of double-positive cells in each group. (**C**) The expression levels of CD80/86 and CD83 in mIgM$^+$ B cells from each in vivo treatment group were assessed by real-time PCR. The relative expression values were averaged from the data in three parallel reactions, and the results were obtained from at least three independent experiments. Flow cytometry was conducted to evaluate the upregulation of mIgM$^+$CD80/86$^+$ (**D**) and mIgM$^+$CD83$^+$ cells (**E**) from sorted mIgM$^+$ B cells upon pulsing with PBS, KLH, and/or LPS for 8 h in vitro. The numbers above the outlined areas indicate the percentages of double-positive cells in each group. (**F**) Real-time PCR analyses were performed to investigate the gene expression of CD80/86 and CD83 in the in vitro PBS–, KLH-, and/or LPS-loaded mIgM$^+$ B cells. Data are mean ± SE from three independent experiments. *$p < 0.05$, **$p < 0.01$.

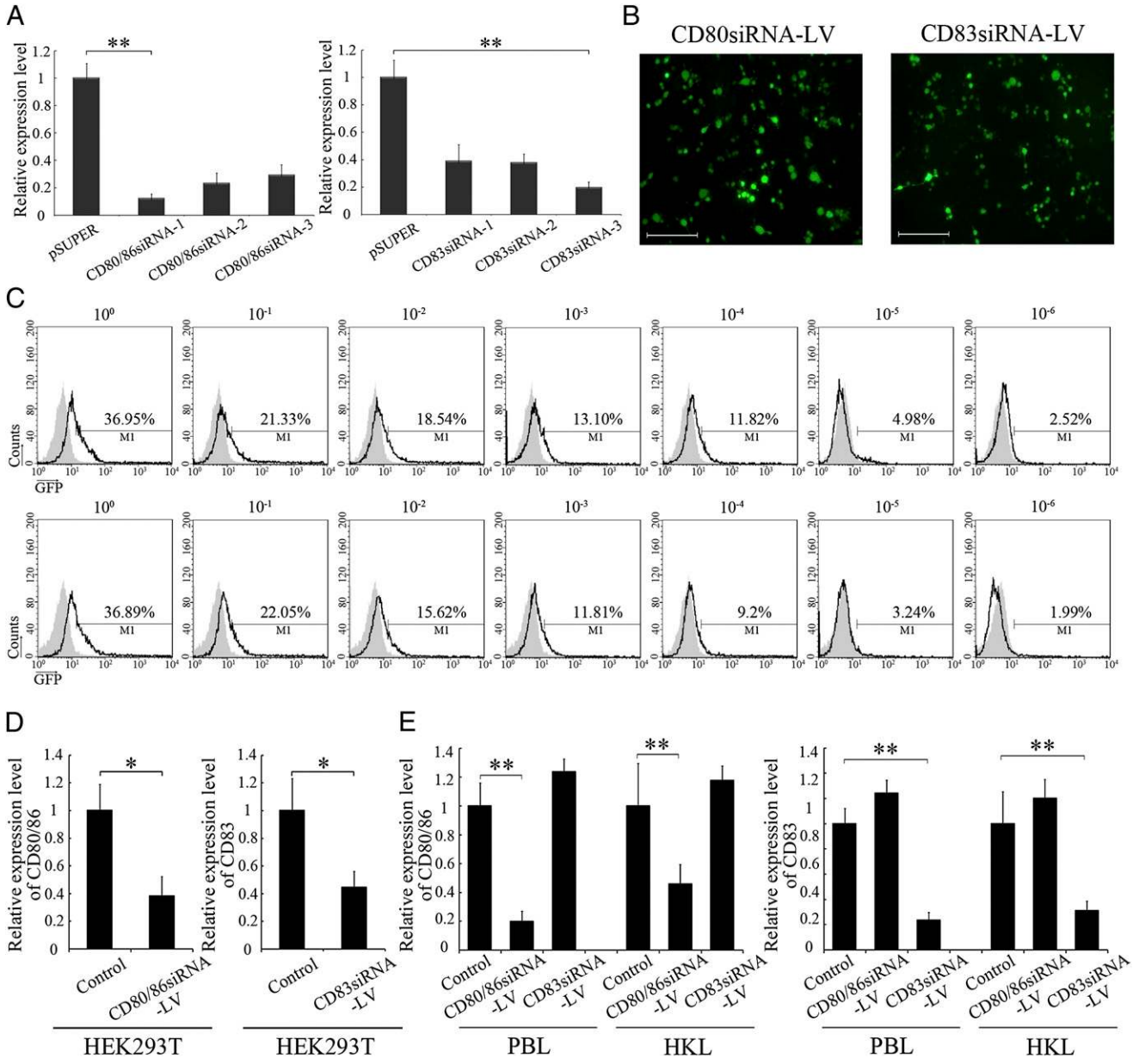

FIGURE 10. Construction of the siRNA-harboring LVs against CD80/86 or CD83. (**A**) Screening of the most effective siRNAs interfering with zebrafish CD80/86 or CD83 expressions. Three designed siRNAs encoding DNA oligonucleotides targeting different regions of each CD80/86 or CD83 mRNA were constructed to pSUPER vectors (pSUPER-CD80/86siRNA-1 to 3 and pSUPER-CD83siRNA-1 to 3), which, in turn, were cotransfected with overexpression pcDNA6-CD80/86 or pcDNA6-CD83 plasmid into HeLa cells. Inhibitory efficiencies were measured by real-time PCR. (**B**) After choosing the most effective siRNAs targeting either CD80/86 or CD83, an LV harboring either of the siRNAs was produced. The infection ability of constructed LVs was evaluated by detecting the GFP fluorescence release in HEK293T cells under a fluorescent microscope (Zeiss Axiovert 40 CFL). Original magnification ×400. Scale bars, 200 μm. (**C**) LV titers were assessed by observing the percentage of GFP$^+$ HEK293T cells after exposure to different dilutions of LVs using flow cytometry. The shaded graphs show background fluorescence on control cells without LV infection. The number above the bracketed line indicates the percentage of cells in each. Data are from three independent experiments. (**D**) The interfering abilities of LVs were investigated in HEK293T cells transfected with the target gene overexpression plasmids in vitro using real-time PCR. (**E**) Detection of the inhibitory effect of CD80/86–siRNA-LV and CD83–siRNA-LV by in vivo administration through real-time PCR analyses. Administration with scrambled siRNA-LV was set as control. Means ± SE from three independent experiments are shown. *$p < 0.05$, **$p < 0.01$.

CD80/86 and CD83 are essential for B cell–initiated CD4$^+$ T cells in vitro

To determine whether zebrafish CD80/86 and CD83 play essential roles in B cell–initiated CD4$^+$ T cell activation, in vitro–blockade assays were conducted using anti-CD80/86 and anti-CD83 Abs. For this, Ag (KLH)-loaded B cells were treated with anti-CD80/86 and anti-CD83 and cocultured with Ag-specific CD4$^+$ T cells (CD4$^+$ T_{KLH}). As shown in Fig. 12A, the proliferation of CD4$^+$ T_{KLH} in response to KLH-loaded B cells decreased significantly ($p < 0.01$) in the blockade groups compared with the nonblockade control groups. Accordingly, the expression levels of Lck and CD154 in the blockade cocultures decreased significantly ($p < 0.01$) (Fig. 12B).

Discussion

Adaptive immunity is generally known to be established in teleost fish based on the origin of Igs and the presence of hallmark molecules and cells necessary for adaptive immunity in higher

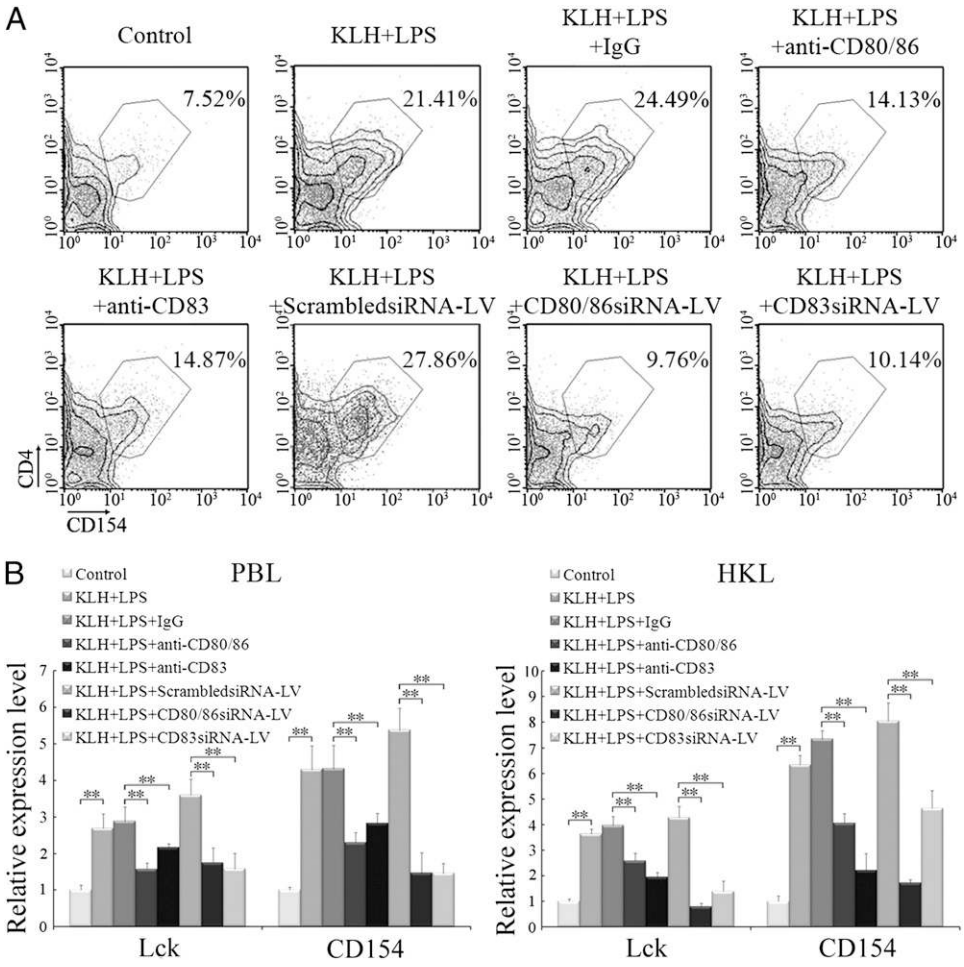

FIGURE 11. In vivo evaluation of CD80/86 and CD83 in $CD4^+$ T cell activation. The degree of $CD4^+$ T cell activation is represented by the percentage of $CD4^+CD154^+$ T cells determined by flow cytometry (**A**) and by the expression levels of Lck and CD154 genes detected by real-time PCR (**B**). For the flow cytometry data, the treatments are presented at the top of each block diagram. The numbers adjacent to the outlined areas indicate the percentages of $CD4^+$ $CD154^+$ cells in each treatment group. For the real-time PCR assay, PCRs were run in combination with the endogenous β-actin control. Error bars represent SE. All data are from at least three independent experiments. $^{**}p <$ 0.01.

vertebrates, such as MHC and T and B cells (25, 47). The B cells in fish were believed to contribute considerably to adaptive immunity because of their ability to produce Abs, such as IgM and IgD (48–50). However, it remains unclear whether fish B cells possess innate-like natures, such as their roles of participation in Ag presentation and initial activation of resting T cells. The recent discovery that teleost B cells have potent phagocytic ability for nonspecific particle Ags and strong microbicidal activity implies that B cells in primitive vertebrates, similar to DCs and macrophages in mammals, may act as pivotal initiating APCs in priming adaptive immunity (4–6). To clarify this hypothesis, direct evidence that B cells in fish can present Ags to initiate naive T cells in the primary adaptive immunity is indispensable. In the current study, we provide such evidence using a zebrafish model based on broad experimental evidence, including phagocytosis, Ag-presentation, in vitro T cell–activation, in vivo B cell–depletion, and adoptive-transfer assays. All of the results support the conclusion that fish B cells can present Ags to prime $CD4^+$ T cells in primary adaptive immunity. It has been known for a long time that the major role of teleost B cells involves Ab secretion, a function pertaining to adaptive immunity (49). However, our present investigation revealed an innate-like function of teleost B cells in the initiation of naive T cells, in addition to their role in adaptive immunity, indicating functional diversification of the ancient B cells. This innate-like nature of primitive B cells puts them forward into the interface that connects innate and adaptive immunity. This innate-like function of primitive B cells enhances the functional understanding of primordial B cells in ancient vertebrates, as well as the evolutionary history of B subsets in modern organisms.

Two B cell subsets, B-1 and B-2, are believed to exist in mammals. B-1 cells are a smaller B cell population residing in the peripheral cavity, producing natural IgM or IgA against T cell–independent Ags. In contrast, B-2 cells are a major B cell population circulating throughout the entire body and producing high-affinity Ag-specific Abs in a T cell–dependent manner (51, 52). As one of the most important cellular components in the immune system, the origin and evolution of B cells have received considerable attention (53, 54). However, this topic has long been challenged in immunology given the limited information about B cells in phylogenetically older species. It was suggested that B cells in mammals originated from primitive phagocytic cells, such as macrophages in ancient vertebrates. This was supported, in part, by the observation that B cells in teleost fish possess potent phagocytic and microbicidal abilities, two innate-like functions typically shared by macrophages (4). Importantly, this finding led to the recent identification of a similar feature shared by B-1 cells in mammals, which points to the innate-like nature of B-1 cells, as well as the existence of a close evolutionary relationship between the ancient B cell lineage and the B-1 subset (10, 11). Given the central function of an innate-like cell in nonspecific Ag presentation, this innate feature has been examined in detail in B-1 cells (53). However, it remains undetermined whether fish B cells have such a function. In the current study, we provide support for such an innate-like nature of fish B cells. Because common phagocytic and Ag-processing and presenting abilities exist among fish B cells, B-1 cells, and innate phagocytic cells, the B-1 cell–like lineage might have originated in teleost fish from a more primitive phagocytic cell, such as macrophages. Moreover, mammalian B-1

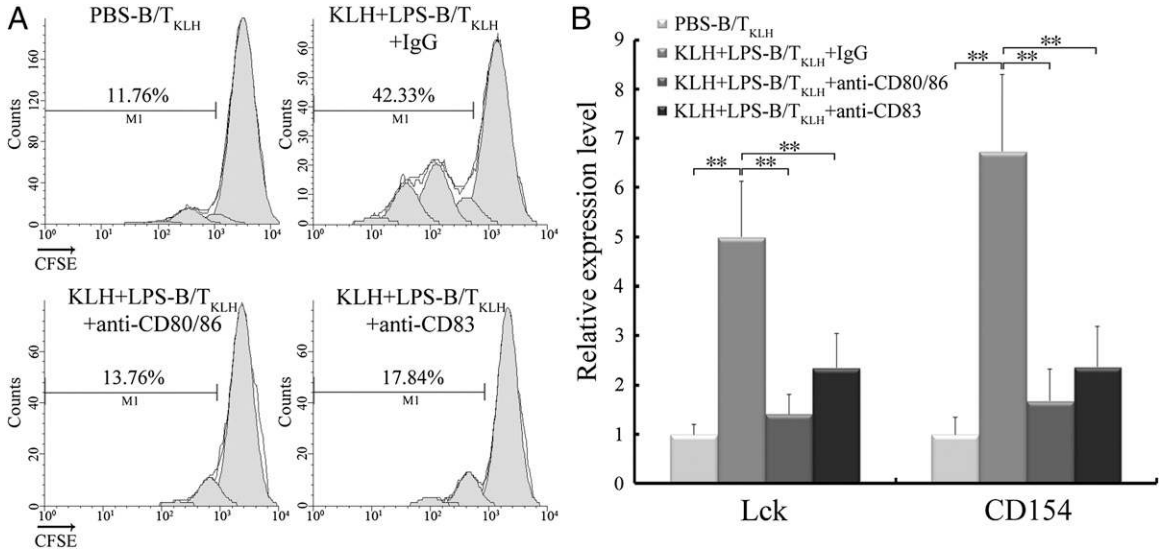

FIGURE 12. CD80/86 and CD83 are essential for B cell–initiated $CD4^+$ T cells in vitro. The inhibition of $mIgM^+$ B cell–mediated $CD4^+$ T_{KLH} proliferation by anti-CD80/86 or anti-CD83 Abs was defined by CFSE dilution measured by flow cytometry (**A**) and by the expression levels of Lck and CD154 detected by real-time PCR (**B**). $CD4^+$ T_{KLH} cells cocultured with PBS-loaded primary $mIgM^+$ B cells were used as control. Error bars represent SE. All data were from at least three independent experiments. $^{**}p < 0.01$.

cells and teleost B cells might originate from a common primordial progenitor, with phagocytic and initiating APC capabilities, in the last common ancestor of teleosts and tetrapods. Two alternative pathways could explain the evolutionary relationship between B-1 and B-2 cell lineages. First, B-2 cells might have originated from a B-1 cell–like lineage, or both B-1 and B-2 cells might have emerged from a common ancient phagocytic cell population. Second, B-2 cells might be derived from a distinct precursor and evolved independently from B-1 cells (9). However, delineation of the exact origin of B-1 and B-2 cells depends on further clarification of the existence of other B cell lineages, as well as the roles and relationships between these B cell lineages in fish and other ectothermic vertebrates (54).

The costimulatory signals provided by CD80, CD86, and CD83 molecules are essential in activating adaptive immunity in mammals. However, whether these signals play similar roles in activating fish adaptive immunity remains poorly understood. In this study, we report the involvement of CD80/86 and CD83 in B cell–initiated adaptive immunity in a zebrafish model. This finding suggests that the costimulatory regulatory mechanism had originated from fish accompanied with the origin of adaptive immunity. Intriguingly, CD80 and CD86 costimulatory molecules exist independently in mammals; however, only a single copy (CD80/86) exists in teleost fish. Thus, it is unclear which homolog, CD80 or CD86, exists in fish. A detailed comparative analysis showed that fish CD80/86 share similar structural features with mammalian CD86, but not with CD80, in terms of both gene organization and protein structures. This finding suggests that the fish CD80/86 molecule might be a homolog of CD86 in mammals. With regard to evolution, CD86 might represent a more primordial costimulatory molecule that initially originated from fish during early vertebrate evolution; however, CD80 might have evolved later from the CD86 ancestor by one gene-duplication event. This suggestion is supported by the considerable amino acid identity, conserved functional domains, and similarity in chromosomal location and organization between these two molecules. In addition, the hypothesis that CD86 is a primordial ancestor is further supported by the recent study (10) showing that CD86, but not CD80, was involved in phagocytic B-1 cell–initiated Ag presentation and T cell activation. Given the existence of a close evolutionary relationship between fish B cells and mammalian B-1 cells, the molecular performance of the costimulatory molecules in B-1 cells may correspondingly occur in fish B cells. Thus, the costimulatory signal in fish B cell–initiated adaptive immunity also may be provided by the CD86 molecule, similar to in B-1 cells. Further comparative analysis between fish B cells and B-1 cells may benefit greatly from the identification and cross-understanding of the molecular and functional evolution of costimulatory signals. For example, mammalian CD80 and CD86 can exert costimulatory function through interaction with a common CD28 receptor. This stimulatory effect can be inhibited by their binding to another common CTLA-4 receptor, which shares higher affinity to CD80 and CD86 than does the CD28 receptor (12, 55). However, the functional divergence between CD80 and CD86 remains elusive. Several investigations showed that CD80 seems to preferentially interact with CTLA-4, largely contributing to the downregulation of Th1 responses and $CD8^+$ T cell activation. In contrast, CD86 prefers to interact with CD28, which is critical for the activation of naive $CD4^+$ T cells in either Th1 or Th2 responses (56, 57). Given that fish lack a CD80 molecule, a more sophisticated CD80-specialized Th1-type and $CD8^+$ T cell response might have evolved from the divergence of CD86 from fish. This hypothesis may be clarified only after the composition and function of $CD4^+$ Th1/Th2 and $CD8^+$ T cell lineages in fish are fully understood and after the relationship of these cell lineages between fish and mammals are determined.

To the best of our knowledge, the current study is the first to prove that teleost B cells can act as pivotal initiating APCs in priming adaptive immunity. This finding suggests that teleost B cells might be a major population of professional APCs whose innate-like function is similar to that of DCs. Functional similarities between teleost B cells and mammalian B-1 cells suggest that the B-1 subset might have originated from a common ancestor with phagocytic and initiating APC capacities. Both CD80/86 and CD83 costimulatory molecules in zebrafish are essential in the B cell–initiated adaptive immune response. Fish CD80/86 resembles mammalian CD86 in both structure and function. It suggests that CD86 might be a more primordial costimulatory molecule that originated from teleost fish as early as the origin

of adaptive immunity. However, CD80 might have evolved later from the CD86 ancestor by one duplication event, accommodating a more CD80-specialized immunity. It is anticipated that our results will be beneficial for fully understanding the origin and evolutionary history of professional APCs, B cell populations, and the costimulatory mechanism underlying adaptive immunity as a whole.

Disclosures

The authors have no financial conflicts of interest.

References

1. Jensen, P. E. 2007. Recent advances in antigen processing and presentation. *Nat. Immunol.* 8: 1041–1048.
2. Chen, X., and P. E. Jensen. 2008. The role of B lymphocytes as antigen-presenting cells. *Arch. Immunol. Ther. Exp. (Warsz.)* 56: 77–83.
3. Ronchese, F., and B. Hausmann. 1993. B lymphocytes in vivo fail to prime naive T cells but can stimulate antigen-experienced T lymphocytes. *J. Exp. Med.* 177: 679–690.
4. Li, J., D. R. Barreda, Y. A. Zhang, H. Boshra, A. E. Gelman, S. Lapatra, L. Tort, and J. O. Sunyer. 2006. B lymphocytes from early vertebrates have potent phagocytic and microbicidal abilities. *Nat. Immunol.* 7: 1116–1124.
5. Øverland, H. S., E. F. Pettersen, A. Rønneseth, and H. I. Wergeland. 2010. Phagocytosis by B-cells and neutrophils in Atlantic salmon (*Salmo salar* L.) and Atlantic cod (*Gadus morhua* L.). *Fish Shellfish Immunol.* 28: 193–204.
6. Zimmerman, L. M., L. A. Vogel, K. A. Edwards, and R. M. Bowden. 2010. Phagocytic B cells in a reptile. *Biol. Lett.* 6: 270–273.
7. Suzuki, K., M. Maruya, S. Kawamoto, and S. Fagarasan. 2010. Roles of B-1 and B-2 cells in innate and acquired IgA-mediated immunity. *Immunol. Rev.* 237: 180–190.
8. Baumgarth, N., J. Chen, O. C. Herman, G. C. Jager, and L. A. Herzenberg. 2000. The role of B-1 and B-2 cells in immune protection from influenza virus infection. *Curr. Top. Microbiol. Immunol.* 252: 163–169.
9. Baumgarth, N. 2011. The double life of a B-1 cell: self-reactivity selects for protective effector functions. *Nat. Rev. Immunol.* 11: 34–46.
10. Parra, D., A. M. Rieger, J. Li, Y. A. Zhang, L. M. Randall, C. A. Hunter, D. R. Barreda, and J. O. Sunyer. 2012. Pivotal advance: peritoneal cavity B-1 B cells have phagocytic and microbicidal capacities and present phagocytosed antigen to CD4+ T cells. *J. Leukoc. Biol.* 91: 525–536.
11. Gao, J., X. Ma, W. Gu, M. Fu, J. An, Y. Xing, T. Gao, W. Li, and Y. Liu. 2012. Novel functions of murine B1 cells: active phagocytic and microbicidal abilities. *Eur. J. Immunol.* 42: 982–992.
12. Chen, L., and D. B. Flies. 2013. Molecular mechanisms of T cell co-stimulation and co-inhibition. *Nat. Rev. Immunol.* 13: 227–242.
13. Paterson, A. M., V. K. Vanguri, and A. H. Sharpe. 2009. SnapShot: B7/CD28 costimulation. *Cell* 137:974–974.e1.
14. Zhou, L. J., R. Schwarting, H. M. Smith, and T. F. Tedder. 1992. A novel cell-surface molecule expressed by human interdigitating reticulum cells, Langerhans cells, and activated lymphocytes is a new member of the Ig superfamily. *J. Immunol.* 149: 735–742.
15. Prechtel, A. T., and A. Steinkasserer. 2007. CD83: an update on functions and prospects of the maturation marker of dendritic cells. *Arch. Dermatol. Res.* 299: 59–69.
16. Rudd, C. E., A. Taylor, and H. Schneider. 2009. CD28 and CTLA-4 coreceptor expression and signal transduction. *Immunol. Rev.* 229: 12–26.
17. Zhang, Y. A., J. Hikima, J. Li, S. E. LaPatra, Y. P. Luo, and J. O. Sunyer. 2009. Conservation of structural and functional features in a primordial CD80/86 molecule from rainbow trout (*Oncorhynchus mykiss*), a primitive teleost fish. *J. Immunol.* 183: 83–96.
18. Hansen, J. D., L. Du Pasquier, M. P. Lefranc, V. Lopez, A. Benmansour, and P. Boudinot. 2009. The B7 family of immunoregulatory receptors: a comparative and evolutionary perspective. *Mol. Immunol.* 46: 457–472.
19. Wittamer, V., J. Y. Bertrand, P. W. Gutschow, and D. Traver. 2011. Characterization of the mononuclear phagocyte system in zebrafish. *Blood* 117: 7126–7135.
20. Ohta, Y., E. Landis, T. Boulay, R. B. Phillips, B. Collet, C. J. Secombes, M. F. Flajnik, and J. D. Hansen. 2004. Homologs of CD83 from elasmobranch and teleost fish. *J. Immunol.* 173: 4553–4560.
21. Haugarvoll, E., J. Thorsen, M. Laane, Q. Huang, and E. O. Koppang. 2006. Melanogenesis and evidence for melanosome transport to the plasma membrane in a CD83 teleost leukocyte cell line. *Pigment Cell Res.* 19: 214–225.
22. Aoki, T., and I. Hirono. 2006. Immune relevant genes of Japanese flounder, *Paralichthys olivaceus*. *Comp. Biochem. Physiol. Part D Genomics Proteomics* 1: 115–121.
23. Doñate, C., N. Roher, J. C. Balasch, L. Ribas, F. W. Goetz, J. V. Planas, L. Tort, and S. MacKenzie. 2007. CD83 expression in sea bream macrophages is a marker for the LPS-induced inflammatory response. *Fish Shellfish Immunol.* 23: 877–885.
24. Hu, Y. H., M. Zhang, and L. Sun. 2010. Expression of *Scophthalmus maximus* CD83 correlates with bacterial infection and antigen stimulation. *Fish Shellfish Immunol.* 29: 608–614.
25. Zhu, L. Y., L. Nie, G. Zhu, L. X. Xiang, and J. Z. Shao. 2013. Advances in research of fish immune-relevant genes: a comparative overview of innate and adaptive immunity in teleosts. *Dev. Comp. Immunol.* 39: 39–62.
26. Hohn, C., and L. Petrie-Hanson. 2012. Rag1$^{-/-}$ mutant zebrafish demonstrate specific protection following bacterial re-exposure. *PLoS ONE* 7: e44451.
27. Monson, C. A., and K. C. Sadler. 2010. Inbreeding depression and outbreeding depression are evident in wild-type zebrafish lines. *Zebrafish* 7: 189–197.
28. Hmama, Z., R. Gabathuler, W. A. Jefferies, G. de Jong, and N. E. Reiner. 1998. Attenuation of HLA-DR expression by mononuclear phagocytes infected with *Mycobacterium tuberculosis* is related to intracellular sequestration of immature class II heterodimers. *J. Immunol.* 161: 4882–4893.
29. Krogh, A., B. Larsson, G. von Heijne, and E. L. Sonnhammer. 2001. Predicting transmembrane protein topology with a hidden Markov model: application to complete genomes. *J. Mol. Biol.* 305: 567–580.
30. Thompson, J. D., T. J. Gibson, F. Plewniak, F. Jeanmougin, and D. G. Higgins. 1997. The CLUSTAL_X windows interface: flexible strategies for multiple sequence alignment aided by quality analysis tools. *Nucleic Acids Res.* 25: 4876–4882.
31. Gong, Y. F., L. X. Xiang, and J. Z. Shao. 2009. CD154-CD40 interactions are essential for thymus-dependent antibody production in zebrafish: insights into the origin of costimulatory pathway in helper T cell-regulated adaptive immunity in early vertebrates. *J. Immunol.* 182: 7749–7762.
32. Lin, A. F., L. X. Xiang, Q. L. Wang, W. R. Dong, Y. F. Gong, and J. Z. Shao. 2009. The DC-SIGN of zebrafish: insights into the existence of a CD209 homologue in a lower vertebrate and its involvement in adaptive immunity. *J. Immunol.* 183: 7398–7410.
33. Wen, Y., W. Fang, L. X. Xiang, R. L. Pan, and J. Z. Shao. 2011. Identification of Treg-like cells in Tetraodon: insight into the origin of regulatory T subsets during early vertebrate evolution. *Cell. Mol. Life Sci.* 68: 2615–2626.
34. Hu, Y. L., X. M. Pan, L. X. Xiang, and J. Z. Shao. 2010. Characterization of C1q in teleosts: insight into the molecular and functional evolution of C1q family and classical pathway. *J. Biol. Chem.* 285: 28777–28786.
35. Zhu, L. Y., P. P. Pan, W. Fang, J. Z. Shao, and L. X. Xiang. 2012. Essential role of IL-4 and IL-4Rα interaction in adaptive immunity of zebrafish: insight into the origin of Th2-like regulatory mechanism in ancient vertebrates. *J. Immunol.* 188: 5571–5584.
36. Traver, D., B. H. Paw, K. D. Poss, W. T. Penberthy, S. Lin, and L. I. Zon. 2003. Transplantation and in vivo imaging of multilineage engraftment in zebrafish bloodless mutants. *Nat. Immunol.* 4: 1238–1246.
37. Hashimoto, K., Y. Maeda, H. Kimura, K. Suzuki, A. Masuda, M. Matsuoka, and M. Makino. 2002. *Mycobacterium leprae* infection in monocyte-derived dendritic cells and its influence on antigen-presenting function. *Infect. Immun.* 70: 5167–5176.
38. Brandes, M., K. Willimann, and B. Moser. 2005. Professional antigen-presentation function by human gammadelta T Cells. *Science* 309: 264–268.
39. Arck, P. C., F. Merali, G. Chaouat, and D. A. Clark. 1996. Inhibition of immunoprotective CD8+ T cells as a basis for stress-triggered substance P-mediated abortion in mice. *Cell. Immunol.* 171: 226–230.
40. Gu, Y. F., Y. Fang, Y. Jin, W. R. Dong, L. X. Xiang, and J. Z. Shao. 2011. Discovery of the DIGIRR gene from teleost fish: a novel Toll-IL-1 receptor family member serving as a negative regulator of IL-1 signaling. *J. Immunol.* 187: 2514–2530.
41. Zhang, R. P., J. Z. Shao, and L. X. Xiang. 2011. GADD45A protein plays an essential role in active DNA demethylation during terminal osteogenic differentiation of adipose-derived mesenchymal stem cells. *J. Biol. Chem.* 286: 41083–41094.
42. Zhang, Y. A., I. Salinas, J. Li, D. Parra, S. Bjork, Z. Xu, S. E. LaPatra, J. Bartholomew, and J. O. Sunyer. 2010. IgT, a primitive immunoglobulin class specialized in mucosal immunity. *Nat. Immunol.* 11: 827–835.
43. Freeman, G. J., G. S. Gray, C. D. Gimmi, D. B. Lombard, L. J. Zhou, M. White, J. D. Fingeroth, J. G. Gribben, and L. M. Nadler. 1991. Structure, expression, and T cell costimulatory activity of the murine homologue of the human B lymphocyte activation antigen B7. *J. Exp. Med.* 174: 625–631.
44. Freeman, G. J., J. G. Gribben, V. A. Boussiotis, J. W. Ng, V. A. Restivo, Jr., L. A. Lombard, G. S. Gray, and L. M. Nadler. 1993. Cloning of B7-2: a CTLA-4 counter-receptor that costimulates human T cell proliferation. *Science* 262: 909–911.
45. Maeda, K., T. Sato, M. Azuma, H. Yagita, and K. Okumura. 1997. Characterization of rat CD80 and CD86 by molecular cloning and mAb. *Int. Immunol.* 9: 993–1000.
46. Terzo, E. A., M. P. de Villarreal, V. Mick, F. Muñoz, B. Amorena, D. de Andrés, and J. M. Pérez de la Lastra. 2006. Molecular cloning of multiple forms of the ovine B7-2 (CD86) costimulatory molecule. *Vet. Immunol. Immunopathol.* 114: 149–158.
47. Lieschke, G. J., and N. S. Trede. 2009. Fish immunology. *Curr. Biol.* 19: R678–R682.
48. Zwollo, P., S. Cole, E. Bromage, and S. Kaattari. 2005. B cell heterogeneity in the teleost kidney: evidence for a maturation gradient from anterior to posterior kidney. *J. Immunol.* 174: 6608–6616.
49. Fillatreau, S., A. Six, S. Magadan, R. Castro, J. O. Sunyer, and P. Boudinot. 2013. The astonishing diversity of Ig classes and B cell repertoires in teleost fish. *Front. Immunol.* 4: 28.
50. Wilson, M., E. Bengtén, N. W. Miller, L. W. Clem, L. Du Pasquier, and G. W. Warr. 1997. A novel chimeric Ig heavy chain from a teleost fish shares similarities to IgD. *Proc. Natl. Acad. Sci. USA* 94: 4593–4597.
51. Strugnell, R. A., and O. L. Wijburg. 2010. The role of secretory antibodies in infection immunity. *Nat. Rev. Microbiol.* 8: 656–667.
52. Su, I., and A. Tarakhovsky. 2000. B-1 cells: orthodox or conformist? *Curr. Opin. Immunol.* 12: 191–194.
53. Parra, D., F. Takizawa, and J. O. Sunyer. 2013. Evolution of B Cell Immunity. *Annu. Rev. Immunol.* 1: 65–97.

54. Sunyer, J. O. 2013. Fishing for mammalian paradigms in the teleost immune system. *Nat. Immunol.* 14: 320–326.
55. Hathcock, K. S., G. Laszlo, C. Pucillo, P. Linsley, and R. J. Hodes. 1994. Comparative analysis of B7-1 and B7-2 costimulatory ligands: expression and function. *J. Exp. Med.* 180: 631–640.
56. Lang, T. J., P. Nguyen, R. Peach, W. C. Gause, and C. S. Via. 2002. In vivo CD86 blockade inhibits CD4+ T cell activation, whereas CD80 blockade potentiates CD8+ T cell activation and CTL effector function. *J. Immunol.* 168: 3786–3792.
57. Sansom, D. M., C. N. Manzotti, and Y. Zheng. 2003. What's the difference between CD80 and CD86? *Trends Immunol.* 24: 314–319.